CHAPTER III

RESULTS AND DISCUSSION

CHAPTER III

RESULTS AND DISCUSSION

III.1.SBA-15 system (pure silica)

III.1.1. X-ray diffraction analysis (XRD)

III.1.1.1 Small-angle XRD studies:

The small-angle XRD patterns of pure SBA-15, Pt /SBA-15 (Fig.9- A) and Ni /SBA-15 (Fig.10- A) catalyst samples with different Pt and Ni concentration, show an intense main well-resolved bragg diffraction peak observed at 2θ ~ 0.85°- 0.89° corresponding to the d_{100} diffraction peak. Another two small peaks assigned to d_{110} and d_{200} at higher 2θ reflections were observed, respectively. The definition of the XRD peaks indicate that the materials have highly ordered mesoporous structures with the hexagonal (P6mm) pore space arrangement.[19, 47]

However, the intensity of the characteristic reflection peak of SBA-15 d_{100} is found to be reduced and vanished with the loading of metals and also as metal concentration increases especially for sample containing 15 wt%Ni providing that NiO is deposited inside the mesopore channels since the attachment of materials to the surface of the mesopore channels tends to reduce the scattering power (or scattering contrast) of the amorphous silicate wall.[133, 134]

Similar behavior was observed previously for the supported Cr/SBA-15 [135] and Co/FSM-16 catalysts.[136] The authors referred such decrease in intensities to the large X-ray mass absorption coefficient of Cr and Co in comparison to those of silicon and oxygen constituting the SiO_2 tetrahedral structure of the supports. Thus, one can apply this explanation to our results in view of the resemblance of Co, Cr, Ni and Pt in their chemical nature.

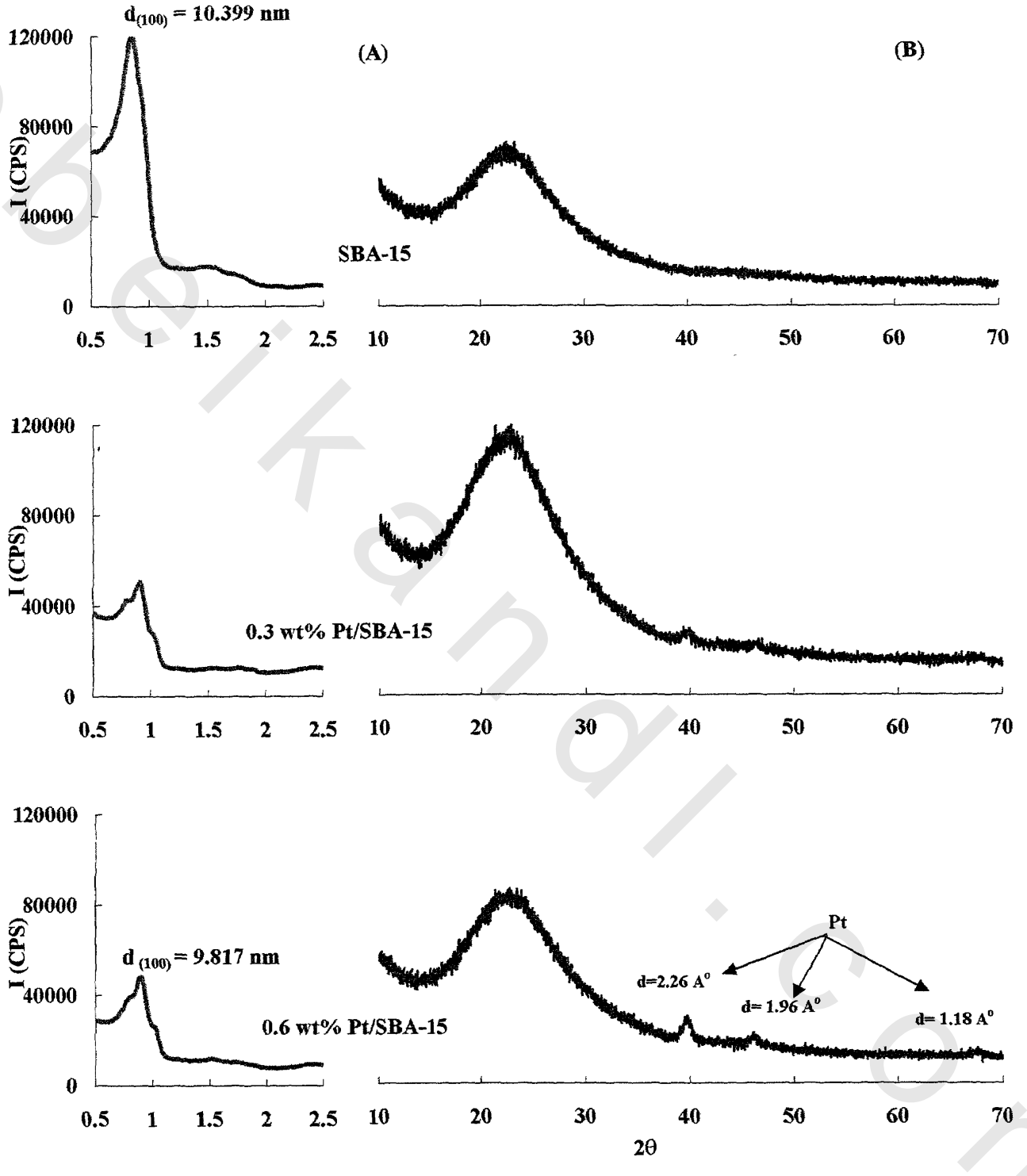

Fig.9 (A) low angle XRD pattern and (B) wide angle XRD pattern of SBA-15 and Pt -supported catalysts

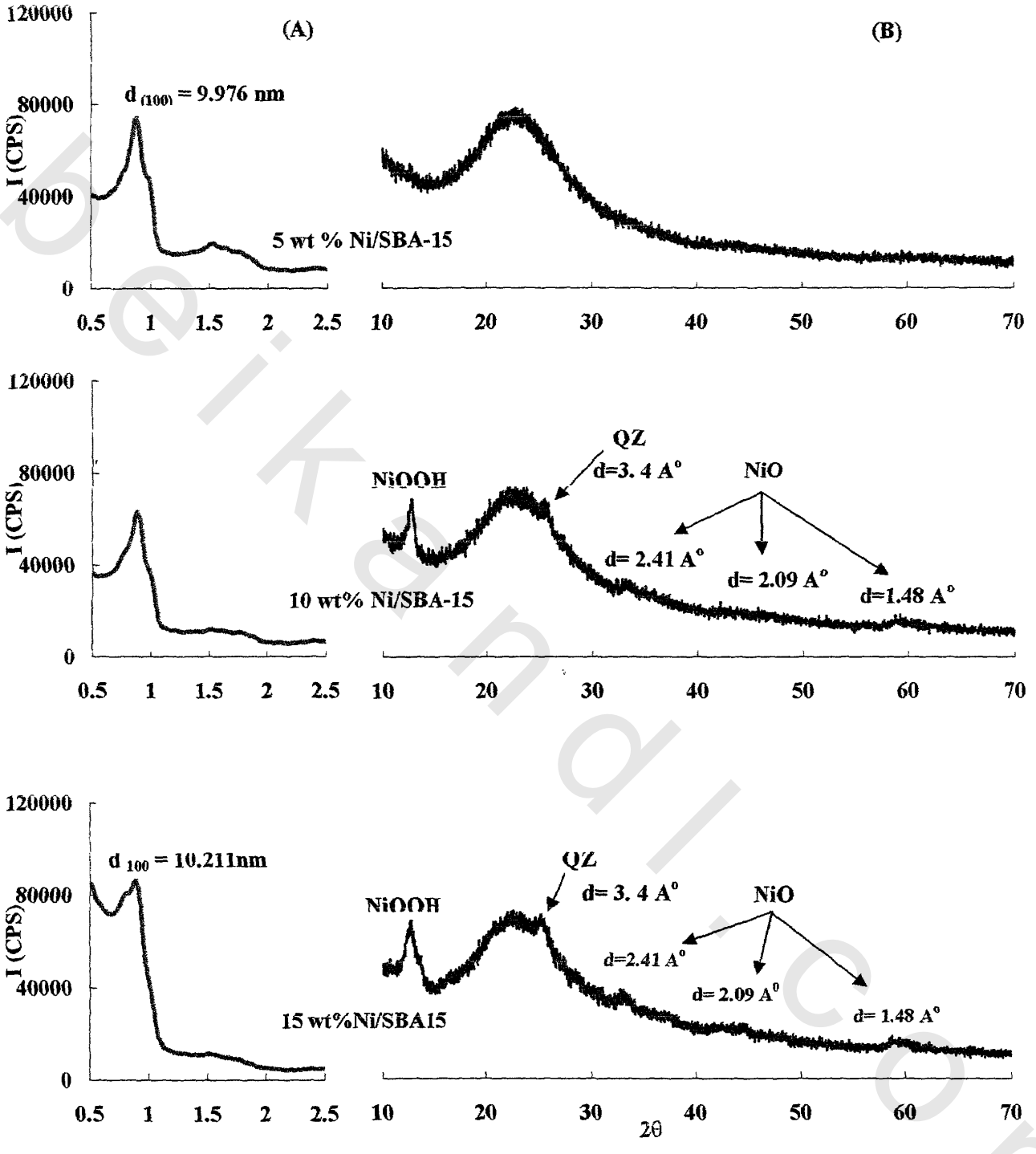

Fig.10 (A) low angle XRD pattern and (B) wide angle XRD pattern of Ni-supported catalysts

The length of the hexagonal unit cell a_o which corresponds to the distance between the centers of adjacent mesopores and d_{100} spacing of the Pt and Ni /SBA-15 samples are shown in Table 1. The unit cell parameters a_o is calculated using the formula ($a_o = 2d_{100}/\sqrt{3}$).[47] This technique was generally accepted as an additional way of establishing the element location in the silicate framework, or as extraframework species.[137]

In general, the incorporation of a larger cation, such as Cr^{3+},Cu^{2+}, Co^{2+} or V^{5+} in a tetrahedral geometry for Si^{4+} is expected to increase to a significant extent the average unit cell (a_o) parameter value.[138]

The observed a_o values for the Pt/SBA-15 and Ni/SBA-15 samples (Table 1) are found to be lower compared with the SBA-15 sample suggesting that these ions are not included within the siliceous matrix but present as an extraframework species. The a_o value decreased as metal content increases. The same behavior was observed for Co/FSM-16 catalysts system.[136] We believe that nickel ions immobilized on the surface of SBA-15 channels by reaction with Si-OH groups of defect sites lead to formation of NiOOH (Fig.10-B) as observed in the wide angle XRD results. This process [139] of immobilized nickel ions reduces the defect sites of the materials, resulting in a more dense structure with a lower a_o value and a reduction of the pore size.

The pore wall thickness (T_{wall}) (Table 1) was assessed by subtracting pore diameter (P.D) from the (a_o) unit-cell parameter. It decreased by platinum and nickel loading if compared with the parent SBA-15 sample (3.912 nm) on the other hand, the sample containing 15 wt% Ni had higher wall thickness than that of pure SBA-15, indicating that the metal cover the walls of the pores increasing their thickness. This behavior was accompanied with decrease in BET surface area, pore volume and average pore diameter (Table 1).

Table 1: Textural parameters of SBA-15, Ni and Pt-supported SBA-15 catalysts

Sample name	BET s.a ($m^2 g^{-1}$)[a]	P.V ($mL g^{-1}$)[b]	P.D (nm)[c]	dV/dD[d]	2θ	$d_{(100)}$ (nm)[e]	a_o (nm)[f]	T_{wall} (nm)[g]
SBA-15	798	1.14	8.095	0.057	0.8488	10.399	12.007	3.912
5 % NiO/SBA -15	587	0.83	7.907	0.046	0.8856	9.976	11.519	3.612
10 % NiO/SBA -15	570	0.80	7.955	0.046	0.8937	9.836	11.357	3.402
15 % NiO/SBA -15	467	0.66	6.144	0.024	0.8645	10.211	11.790	5.646
0. 3 % PtO/SBA -15	672	0.93	8.068	0.055	0.8300	9.652	11.145	3.077
0. 6 % PtO/SBA -15	463	0.85	7.923	0.053	0.8991	9.817	11.335	3.412

a: Surface area calculated from BET equation.
b: Pore volume calculated from the adsorption branch of isotherm at P/Po ~ 0.98.
c: Pore diameter calculated from the adsorption branch of the isotherm according to BJH method.
d: Obtained from pore size distribution curve at the apex of the pattern.
e: d spacing from XRD.
f: Unit cell parameters calculated using formula $a_o = 2d_{100}/\sqrt{3}$.
g: wall thickness calculated from the difference between a_o and pore diameter.

In addition, the d_{110} and d_{200} peaks become faint and diffuse as nickel percent increase especially for sample contain 15 wt% Ni and for 0.3 and 0.6 wt% Pt/SBA-15 catalyst samples, which indicates that the modification process seems to obviously influence the mesoporous channels. Similar results had been previously observed in the metal modified mesoporous silica materials.[140, 141]

III.1.1.2. Wide-angle XRD studies:

The wide-angle XRD patterns (Figs.9 and 10- B) for all of these samples show a broad hump due to amorphous silica. It should be noted that these x-ray diffractograms are identical to the traditional pattern of amorphous silica gel.[142]

In the wide-angle XRD of Pt/SBA-15 (Fig 9-B) shows reflections of the large Pt particles at 2θ of 39.8°; 46.2° and 67.4° which can be attributed to (111), (200) and (220) inter planar spacings of the cubic platinum metal structure, respectively.[143] Their intensities increased with increasing Pt concentration (0.3 – 0.6wt %).

NiOOH (d= 6.9 Å), quartz (d = 3.4 Å) and NiO (d =2.41 Å) were clearly observed in Ni/SBA-15 sample diffractograms (Fig.10-B) whose intensities increased as nickel loading increase.

NiOOH at d-spacing = 6.9 Å of (ICDD-JCPDS card no.06-0075) may be formed due to the interaction between NiO with free silanol groups of SBA-15 support. The intensity of the peak corresponding to NiOOH increase by nickel loading (5- 15wt %); this is also supplemented by DSC-TGA result.

For the sample containing ≥10 wt% Ni, a quartz phase (SiO_2, at d spacing = 3.4Å) was clearly observed. This behavior may be explained on the basis that the nickel species act as modifying agent (i.e. seems to have some catalyzing effect) on the silica structure (Si–O–Si) leads to increase or decrease of silica crystallinity according to critical nickel concentration. This means that 15% Ni is the most suitable concentration to form of quartz phase. Similar observation was noticed for 11 % Ag/Silica gel in previous work.[144] Another reason for the formation of quartz may be due to nitrate precursor solution act as an oxidizing agent which effect on the silanol group and recrystalize amorphous silica to crystalline one (quartz).

III.1.2.Surface Characteristics

The nitrogen adsorption–desorption isotherms and the corresponding pore-size distribution curves of pure SBA-15 support, Ni/SBA-15 and Pt/SBA-15 catalysts are shown in Figs. 11, 12 and 13, respectively.

The isotherms of SBA-15 and catalyst samples correspond, according to IUPAC classification,[1] to a typical irreversible type IV isotherm with H1 hysteresis at $P/P^o > 0.6$, characteristic of capillary condensation inside uniform cylindrical pores. The P/P^o position of the inflection points is related to the diameter in the mesoporous range and the sharpness of the step indicates uniformity in the pore size distribution.

The shape of N_2 adsorption–desorption isotherm of nickel and platinum containing SBA-15 are similar to that of the pure SBA-15, indicating that the mesoporous structure of SBA-15 is mostly retained upon nickel and platinum impregnation.

Impregnation of Ni and Pt did not change the pore size distribution peak shape and position; indicating that the hexagonal array of pores was well preserved after the incorporation except that the peak height was smaller and shifted to lower D (nm) value for catalyst sample containing 15 wt% Ni, which means some decrease in pore volume by the incorporation of Ni particles inside the mesopores and the average pore diameter decreased by the deposition of Ni on the pore walls.

The capillary condensation areas become shallower and smaller for 15%Ni/SBA-15 sample and for samples containing 0.3 and 0.6%Pt /SBA-15.

In Table 1, it is apparent that the loading of active component has a notable impact on the surface area of mesoporous SBA-15. The specific surface area, pore volume and average pore diameter of SBA-15 dropped appreciably with 15 wt%Ni and 0.6 wt% Pt loaded on SBA-15 catalysts as the result of the deposition of nickel oxide (NiO) via wetness impregnation method. In the wetness impregnation method, NiO is usually deposited on the mesoporous silica in an irregular manner,[145] thus blocking some of the pore channels of the bare SBA-15. A substantial loss in the BET surface area and the total pore volume for 0.6 wt % Pt is mainly caused by the partial blockage of the SBA-15 pores.

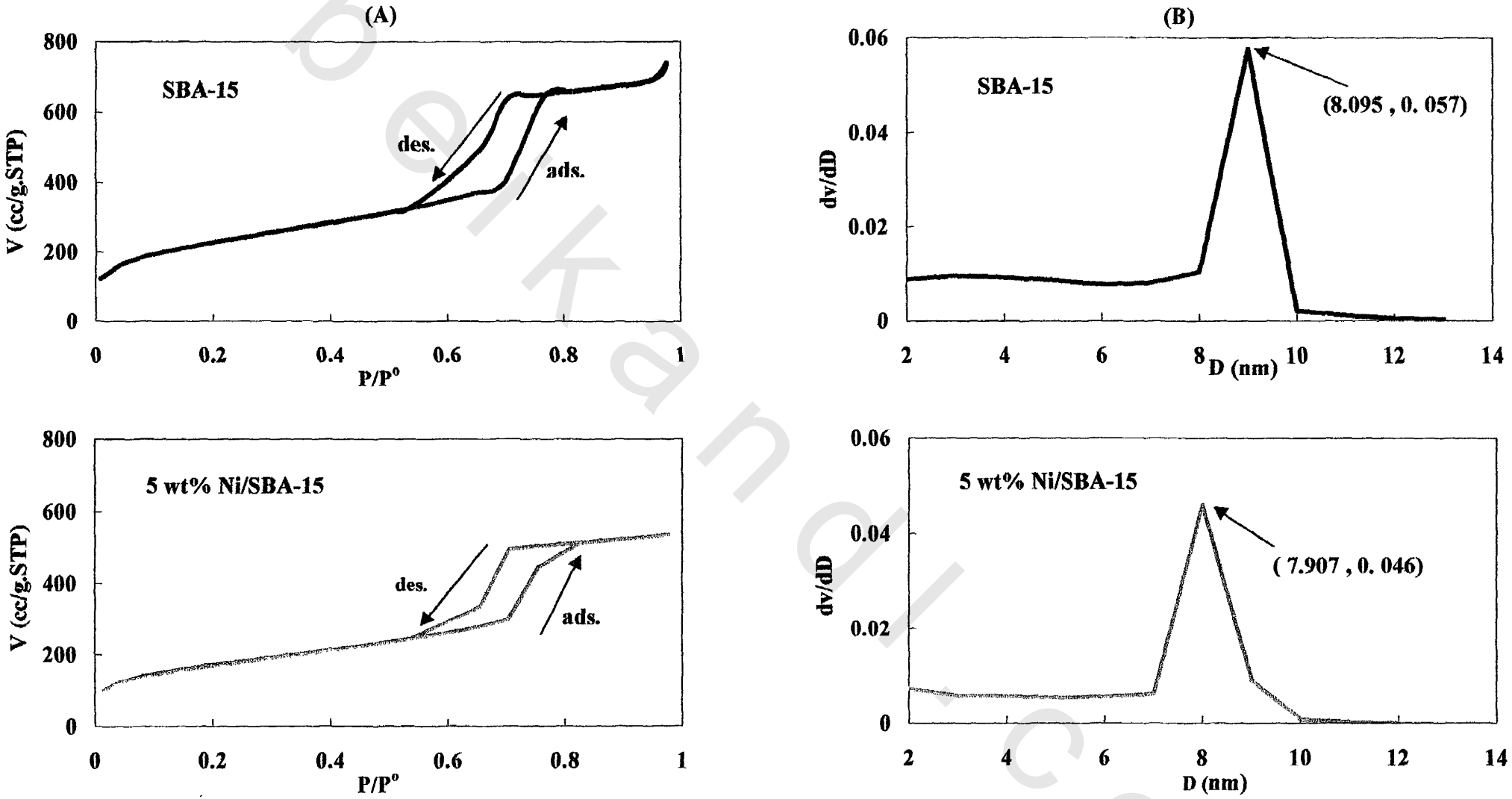

Fig.11 (A) the Nitrogen adsorption - desorption isotherms and (B) Pore Size Distrbution curves of SBA-15 and Ni/SBA-15 catalyst

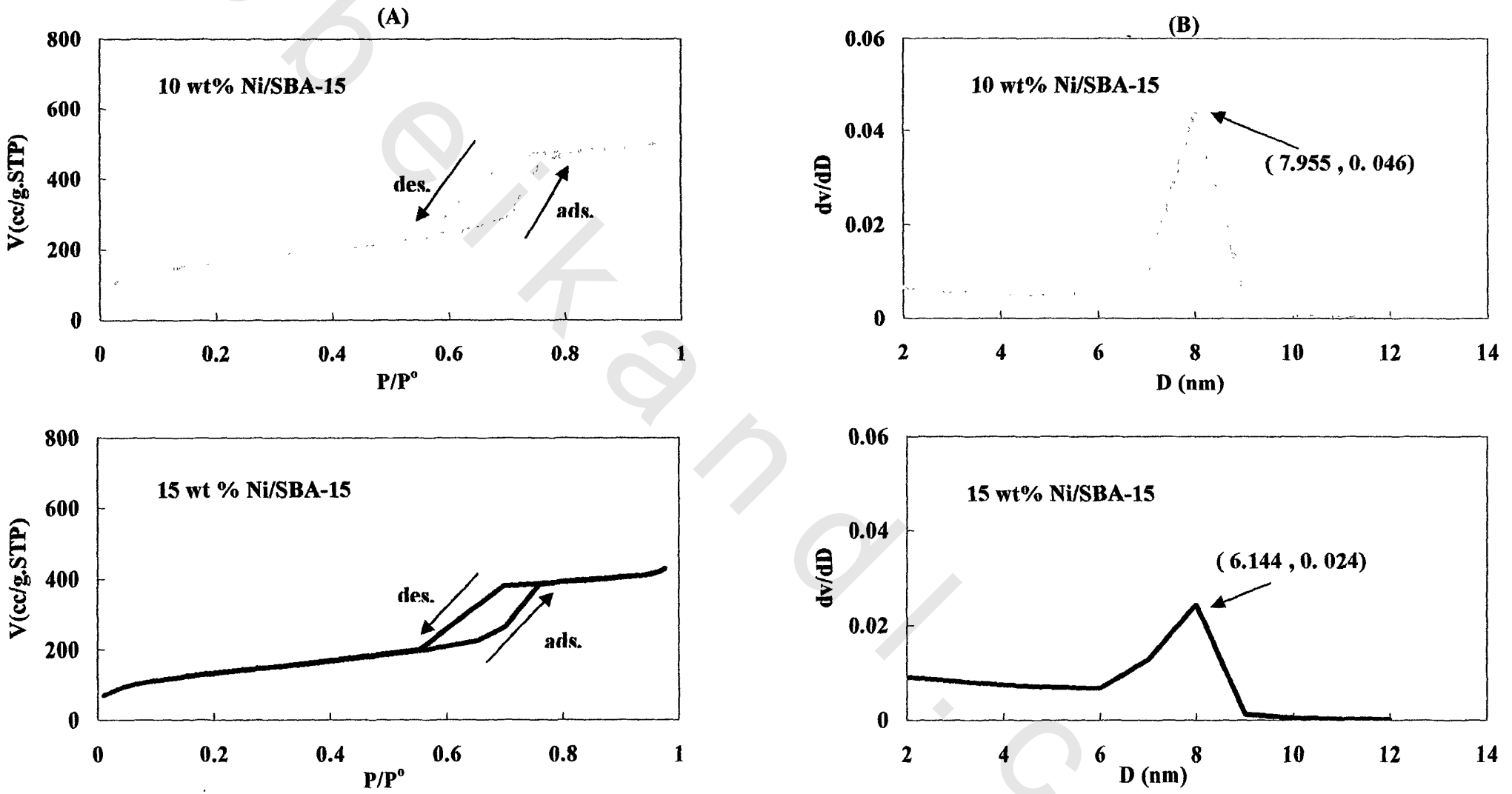

Fig.12 (A) the Nitrogen adsorption - desorption isotherms and (B) Pore Size Distribution curves of Ni/SBA-15 catalysts

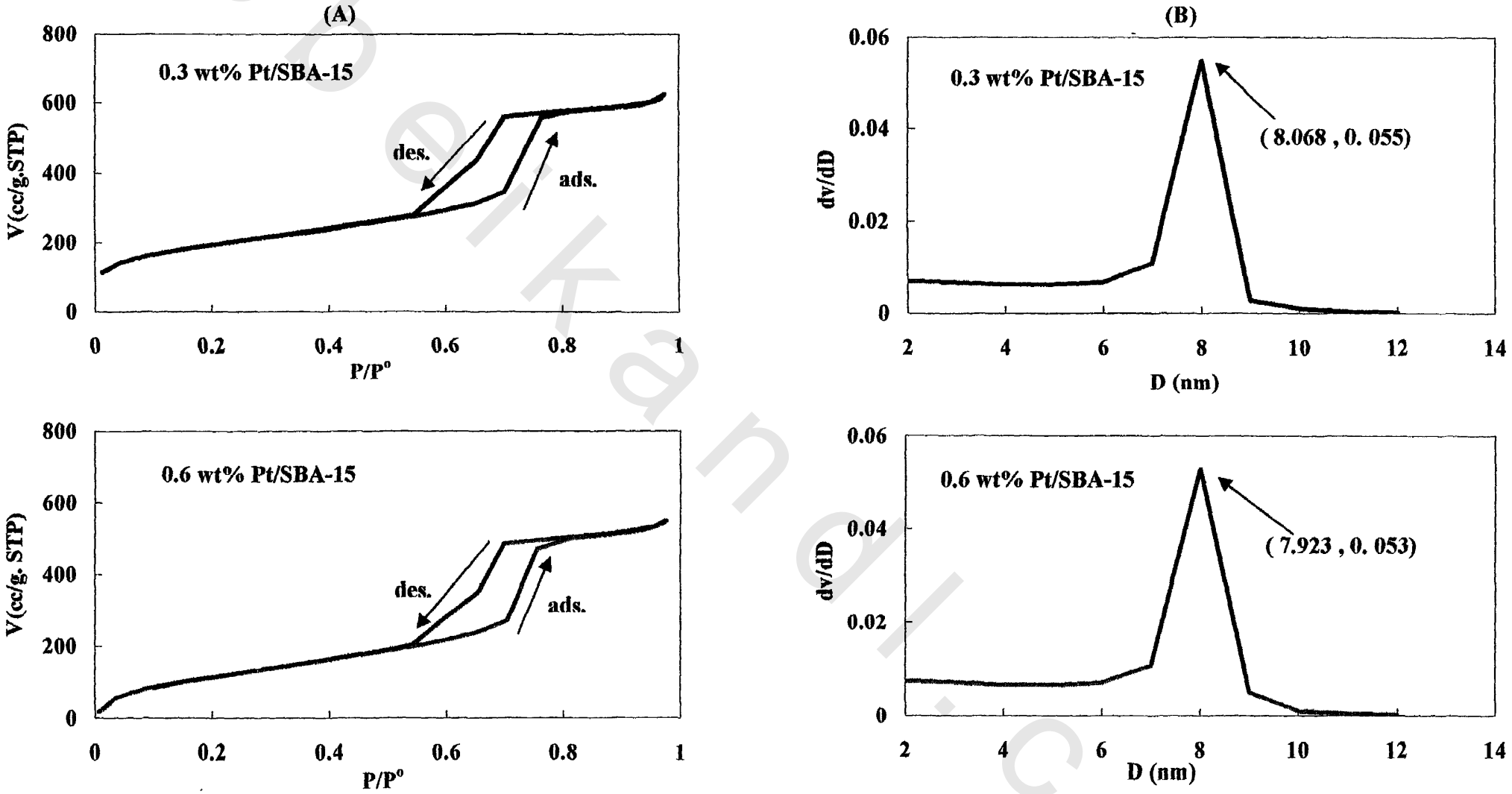

Fig.13 (A) Nitrogen adsorption-desorption isotherms of and (B) Pore Size Distribution curves of Pt/SBA-15 catalysts

III.1.3.Thermal Analysis

DSC analysis is heating the sample linearly where endo- and exothermic events takes place. The intensity of the resulted peaks is measure of heat flow dH/dt (rate of energy change per unit time). TGA analysis is technique that measures the weight loss (or weight gain) of a material as a function of temperature.

Pure SBA-15 mesoporous material (Figs.14 and 15 –A) and Table 2 shows one endothermic peak at $T_{max.}$ ~ 50 °C. This event is attributed to the dehydration of physisorbed water.

By loading SBA-15 support with 5, 10, 15 wt% Ni and 0.3, 0.6 wt%Pt, this peak shifted to higher temperature, $T_{max.}$ ~ 60 – 80 °C, Table 2. This event is accompanied by weight loss as detected by TGA (Figs. 14 and 15 -B) and Table 2.

ΔH and ΔS of the first dehydration event (Table 2) are increased (12.6 – 33.4 cal. /g) as nickel loading increases (5 – 15 wt% Ni). This means that the process became difficult with loading due to formation of more NiOOH on the surface (surface crowdness increases) which renders water dehydration more difficult. Also NiOOH act as new adsorbent with strong hydrogen bonding between NiOOH and adsorbed water molecules, especially for the sample containing 15 wt%Ni. The same behavior was observed for Pt/SBA-15 samples but the ΔH value and weight loss are almost the same for samples contain 0.3 and 0.6 wt %Pt.

Beside the physisorbed peak of SBA-15, the nickel loaded samples only, show second endothermic peak (Fig.14-A) accompanied with weight loss (Fig.14-B) and Table 2 which become more pronounced as nickel content increases. This event corresponds to the dehydroxylation of OH present in NiOOH phase resulting from metal-support interaction. This confirms the XRD data. This event is not present in DSC pattern of Pt/SBA-15 samples (Fig.15-A) due to there is not present interaction between support and platinum.

The dehydroxylation process of OH from NiOOH (second event) is easier than the dehydration process (first event) of physisorbed water according to the ΔH, Cp and ΔS values of both processes (Table 2).

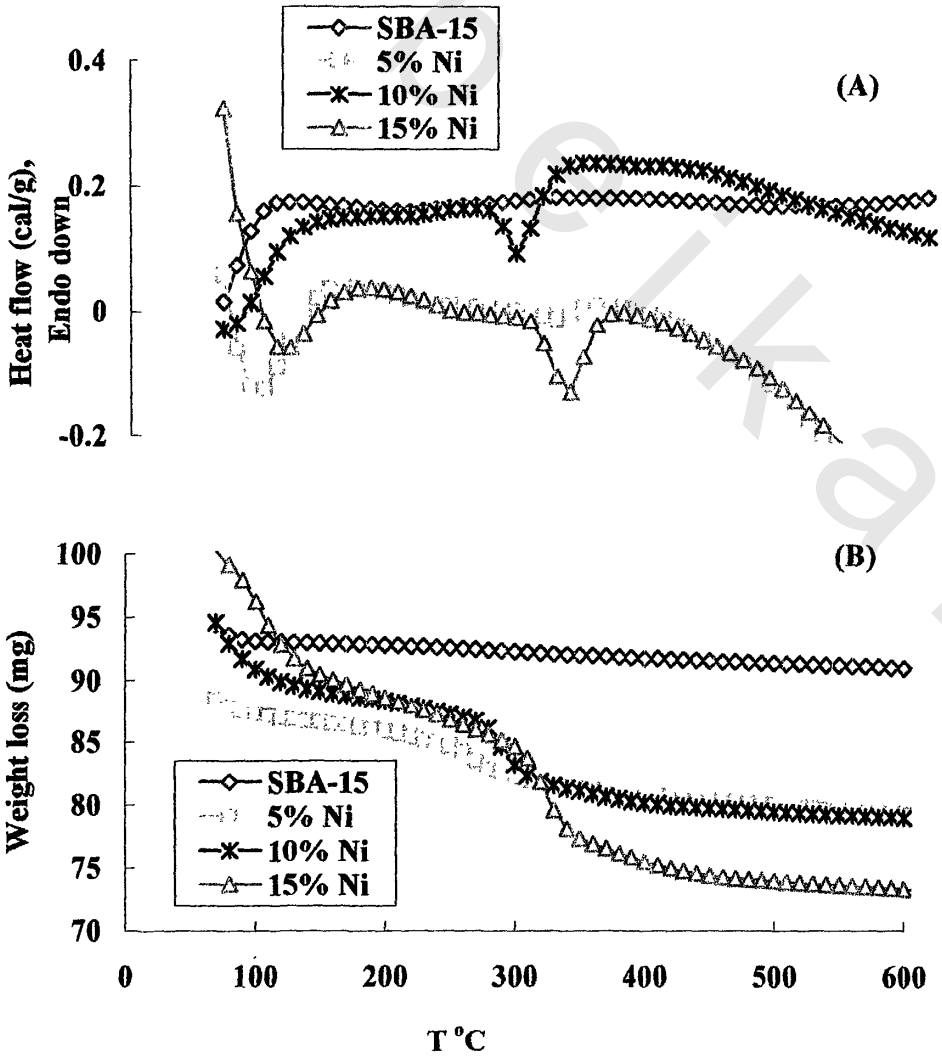

Fig.14 (A) DSC and (B) TGA curves of SBA-15 and Ni /SBA-15 catalysts

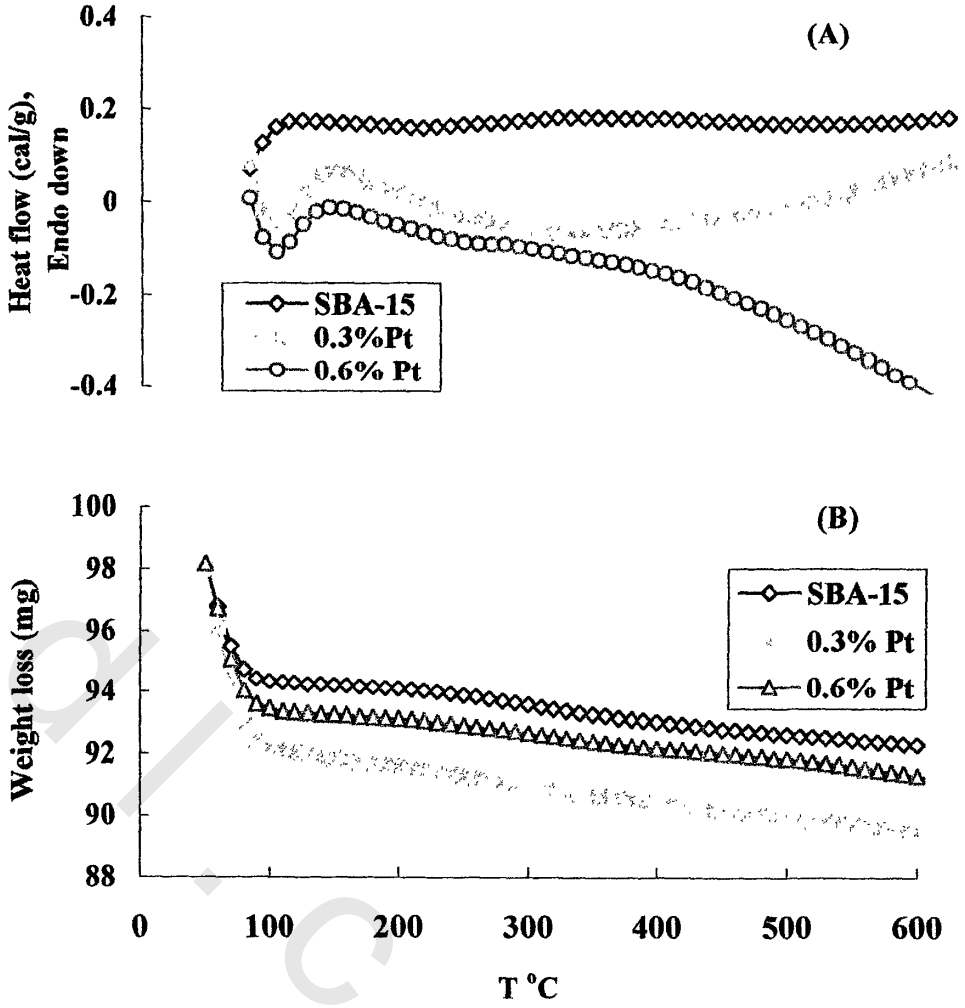

Fig.15 (A) DSC and (B) TGA curves of SBA-15 and Pt /SBA-15 catalysts

Table 2: DSC and TGA of SBA-15, Ni and Pt-supported SBA-15 catalysts

Sample name	1st event							2nd event						
	T_1 (°C)	T_2 (°C)	$T_{max.}$ (°C)	ΔH (Cal/g)	wt loss (mg)	Cp (Cal/g . deg)	ΔS (Cal/g . deg)	T_1 (°C)	T_2 (°C)	$T_{max.}$ (°C)	ΔH (Cal/g)	wt loss (mg)	Cp (Cal/g . deg)	ΔS (Cal/g . deg)
SBA-15	30	100	50	8.0	0.32	0.12	0.14	-	-	-	-	-	-	-
5%Ni	40	110	60	12.6	0.58	0.18	0.18	270	310	290	2.2	0.16	0.06	0.03
10%Ni	40	120	60	28.1	0.50	0.35	0.39	260	320	280	13.7	0.31	0.23	0.05
15%Ni	40	120	80	33.4	0.50	0.47	0.52	260	320	290	19.7	0.46	0.33	0.07
0.3%Pt	40	90	60	21.9	0.34	0.41	0.33	-	-	-	-	-	-	-
0.6%Pt	40	100	60	23.8	0.38	0.39	0.36	-	-	-	-	-	-	

III.1.4.Catalytic Activity

Petroleum wax composed mainly from paraffin compounds. In our search we study the catalytic activity of the prepared catalysts using model compounds as cyclohexane and n-hexane to illustrate which one is suitable for hydroconversion (hydrocracking and hydroisomerization) of paraffins. This part deals with the effect of the metals (5, 10 and 15 wt% Ni) and (0.3 and 0.6wt% Pt), and the support (SBA-15) on the catalytic processes.

III.1.4.1.Catalytic activity of Pt/SBA-15 catalysts

(A) Cyclohexane conversion

The Catalytic conversion of cyclohexane over Pt/SBA-15 catalyst samples containing 0.3 And 0.6 wt%Pt/SBA-15 were shown in Fig.16 (A and B) and Table 3.

It is observed that the dehydrogenation activity of 0.6 wt% Pt/SBA-15 catalyst is much higher than 0.3 wt % Pt/SBA-15. Benzene yield (mole %) is sharply increases with temperature and reaches 100% at 350 for 0.6 wt% Pt/SBA-15 catalyst if it is compared with 0.3 wt % Pt/SBA-15 sample (45%).

The selectivity of benzene formation (Fig.16-A and B), achieves a constant maximum value of 100% over whole range of temperature (250-450 °C). This behavior reflects that the 0.6 wt%PtSBA-15 is active and selective catalyst for cyclohexane dehydrogenation into benzene. No sign of presence of cracking side reaction takes place under the operating conditions.

(B) n-hexane conversion

Pt/SBA-15 catalyst samples containing 0.3 and 0.6 wt%Pt/SBA-15 didn't show any catalytic activity toward n-hexane conversion.

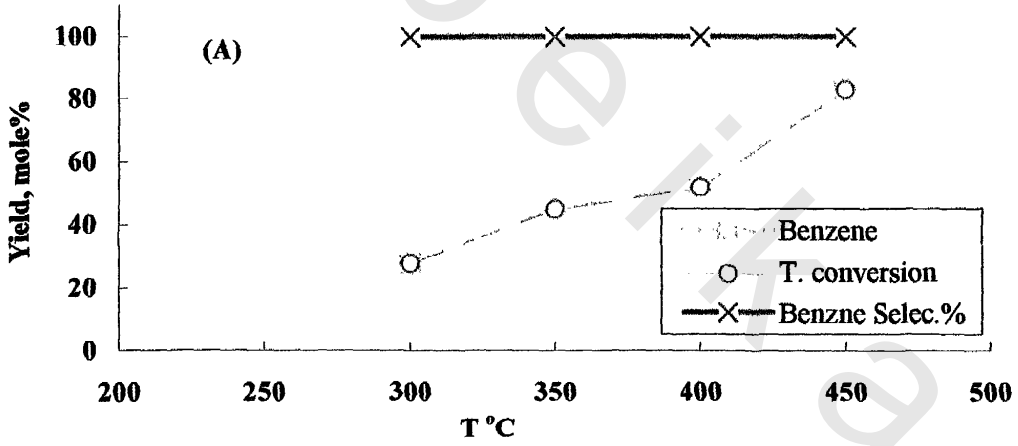

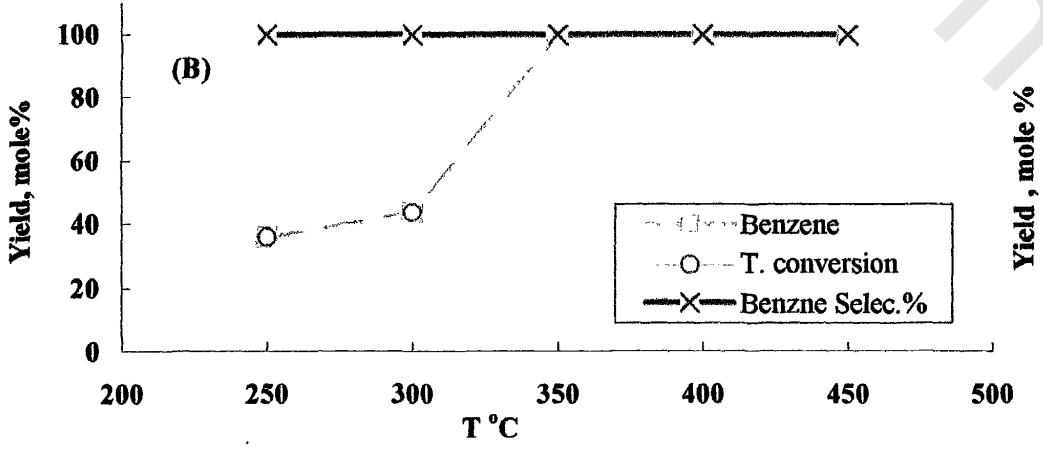

Fig. 16 The catalytic conversion of cyclohexane over Pt / SBA-15 catalysts: (A) 0.3 wt% Pt and (B) 0.6 wt% Pt

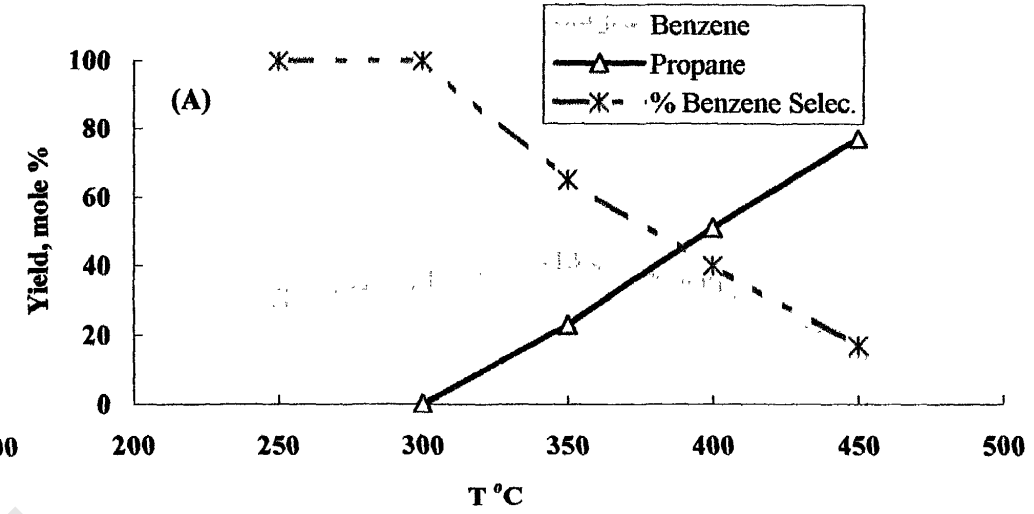

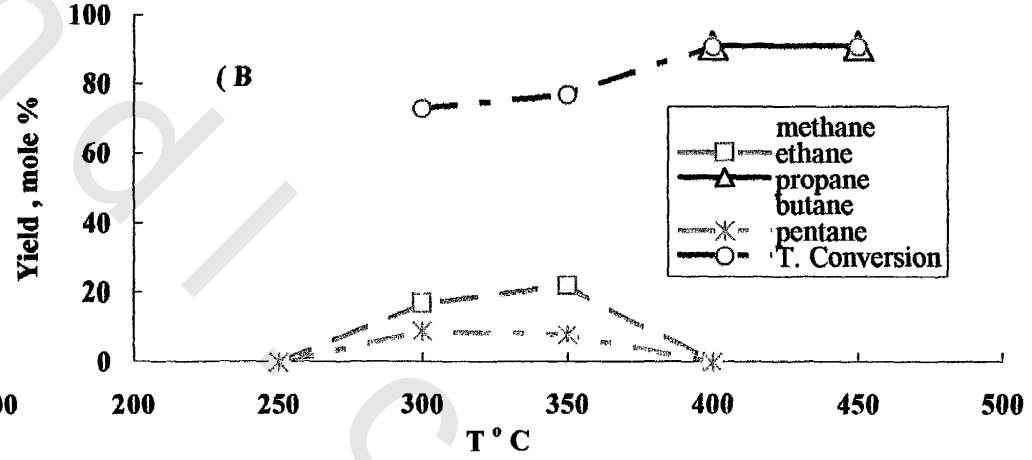

Fig. 17 The catalytic conversion of (A) cyclohexane (B) n-hexa over 5 wt% Ni/SBA-15

Table 3: Catalytic conversion of cyclohexane over Pt / SBA-15 catalysts: (A) 0.3 wt%Pt and (B) 0.6 wt%Pt

Reaction products	Reaction temperature, ^{O}C				
(A)	250	300	350	400	450
Benzene	0	28	45	52	83
Cyclohexane	100	72	55	48	17
T.conversion	0	28	45	52	83
Benzene selc. %	100	100	100	100	100
(B) Benzene	44	100	100	100	100
Cyclohexane	56	0	0	0	0
T.conversion	44	100	100	100	100
Benzene selc. %	100	100	100	100	100

Table 4: Catalytic conversion of cyclohexane over Ni/SBA-15 catalysts: (A) 5 wt% Ni (B) 10 wt% Ni and (C) 15 wt%Ni

Reaction products	Reaction temperature, ^{O}C				
(A)	250	300	350	400	450
Benzene	31	36	42	34	16
propane	0	0	23	51	77
cyclohexane	69	64	35	15	7
T.conversion	31	36	65	85	93
(B) Benzene	5	53	36	15	13
propane	0	2	43	82	87
cyclohexane	95	45	21	3	0
T.conversion	5	55	79	97	100
(C) Benzene	17	46	22	16	4
propane	0	9	65	74	92
cyclohexane	83	45	13	10	4
T.conversion	17	55	87	90	96

III.1.4.2.Catalytic activity of Ni/SBA-15 catalysts

(A) Cyclohexane conversion

The catalytic conversion of cyclohexane over Ni/SBA-15 catalyst samples containing 5, 10 and 15 wt%Ni/SBA-15 were shown in (Figs. 17, 18 and 19 –A) and Table 4.

The benzene yield increases with temperature reaching a maximum at 300 °C, 5 wt % Ni (36%) , 10 wt % Ni (53%) and 15 wt % Ni (46%) and then declines due to the appearance of gaseous cracking products which is mainly propane. The selectivity of benzene formation decreases with both temperature and nickel loading. The yield of cyclohexane cracking into propane (Figs. 17, 18 and 19-A) is increased at expense of benzene formation with increasing both reaction temperature and nickel concentration. The cracking yield reaches 77, 87 and 92 % at 450 °C for 5, 10 and 15 wt % Ni, respectively.

(B) n-hexane conversion

The catalytic conversion of n-hexane over Ni/SBA-15 catalysts with different Ni loading (Figs. 17, 18 and 19 -B) and Table 5 gives rise to many cracking products such as (methane, ethane, propane, butane and pentane).

The yield of each reaction increases slightly by temperature. However n-hexane cracking into propane shows highest yield in comparison with other cracking products, which reach ~ 100 yield at 450 °C for all nickel catalyst samples. Total conversion n-hexane cracking (Fig. 17, 18 and 19-B) increases by nickel loading.

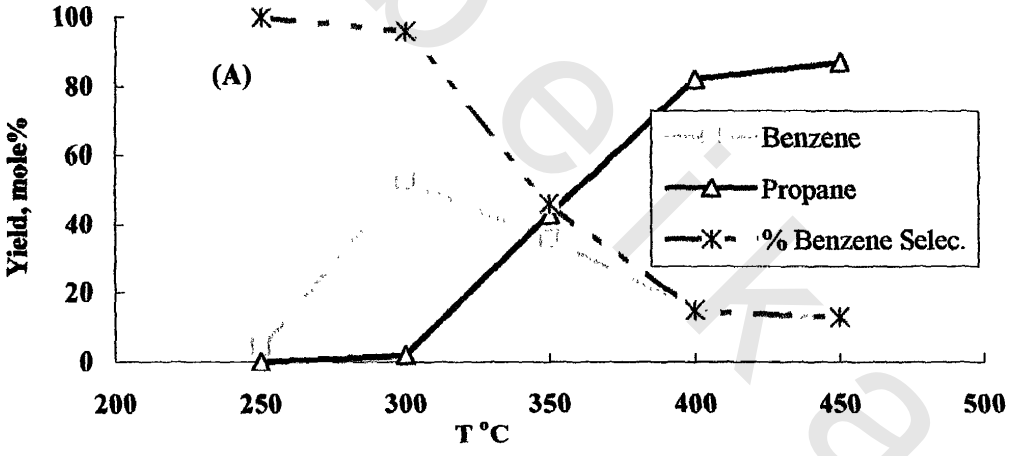

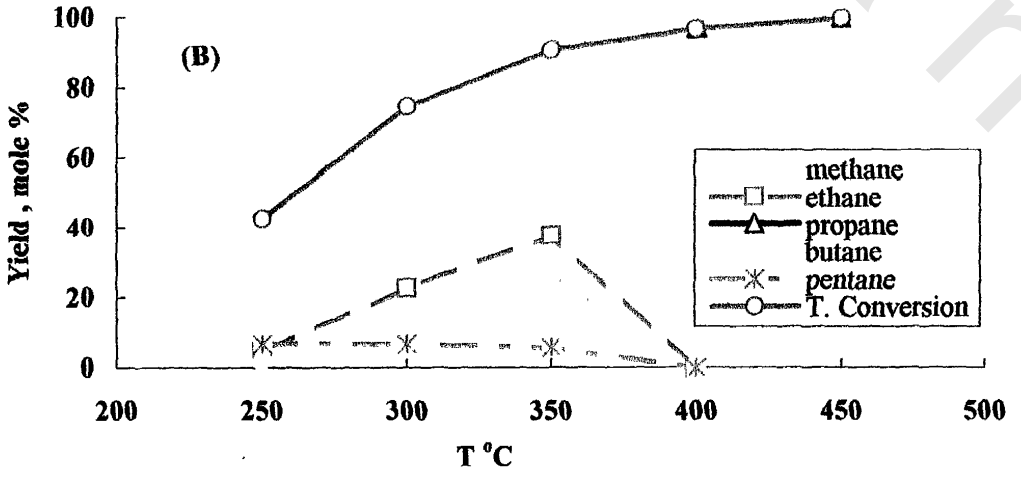

Fig.18 The catalytic conversion of (A) cyclohexane (B) n-hexane over 10 wt% Ni / SBA-15

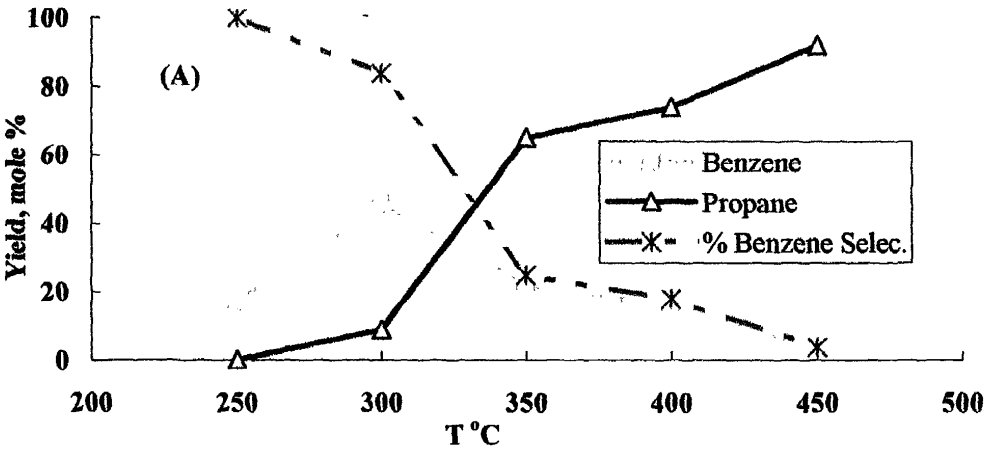

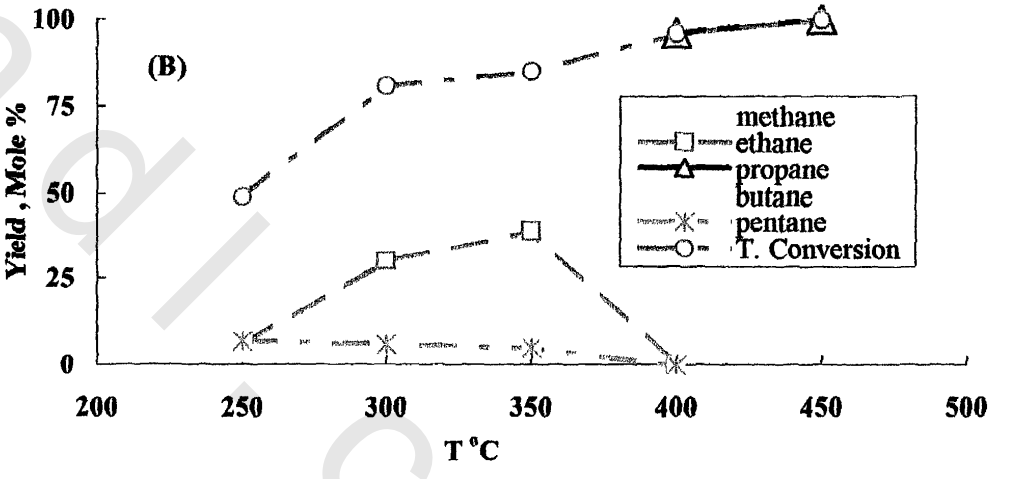

Fig.19 The catalytic conversion of (A) cyclohexane (B) n-hexane over 15 wt% Ni / SBA-15

Table 5: Catalytic conversion of n-hexane over Ni /SBA-15 catalysts: (A) 5 wt%Ni (B) 10 wt%Ni and (C) 15 wt% Ni

Reaction product	Reaction temperature, ^{O}C				
(A)	250	300	350	400	450
methane	0	38	36	0	0
ethane	0	17	22	0	0
propane	0	0	0	91	91
butane	0	9	11	0	0
pentane	0	9	8	0	0
n-hexane	100	27	23	9	9
T.conversion	0	73	77	91	91
(B) methane	29	33	27	0	0
ethane	5	23	38	0	0
propane	0	0	0	97	100
butane	2	12	20	0	0
pentane	7	7	6	0	0
n-hexane	57	25	9	3	0
T.conversion	43	75	91	97	100
(C) methane	33	29	21	0	0
ethane	6	30	39	0	0
propane	0	0	0	96	100
butane	3	16	20	0	0
pentane	7	6	5	0	0
n-hexane	51	19	15	4	0
T.conversion	49	81	85	96	100

-In conclusion, Pt/SBA-15 catalysts are selective ones for dehydrogenation of cyclohexane into benzene that occurs mainly on Pt metallic particles of the catalyst. On the other hand, Ni/ SBA-15 catalyst samples exhibit higher cracking activity, which increases by increasing the nickel loading and reaction temperature. The cracking activity seems to result from the produced NiOOH species, especially in the sample of high nickel content (viz., 15wt %) may be responsible for this cracking activity (Refer to XRD results).

- It is obvious that neither Pt/SBA-15 nor Ni/SBA-15 catalyst samples gave rise to n-hexane hydroconversion which probably attributed to lake of acidity of SBA-15 support. So another work concerning in the study of n-hexane hydroconversion will be examined on Ni and Pt-supported AlSBA-15 catalyst samples.

III.2. AlSBA-15 system

III.2.1. X-ray diffraction analysis (XRD)

III.2.1.1. Small-angle XRD studies:

The small-angle XRD patterns of the prepared AlSBA-15(5, 7 and 14) and their corresponding Ni and Pt-supported catalysts showed typical mesoporous structures (Figs. 20-25–A) in accordance with those reported in literature.[47] These materials exhibit one strong reflection d_{100} at $2\theta \sim 0.69^{o} - 0.87^{o}$ and two weaker peaks d_{110}, d_{200} at higher 2θ, associated with the hexagonal symmetry and like wise characteristic of the 2D hexagonal ordered structure. The shape of the powder XRD patterns of AlSBA-15 samples is almost similar to that of the parent mesoporous silica SBA-15 (Fig.9-A), indicating that the hexagonally ordered two dimensional honey comb type of the parent silica structure is retained even after the incorporation of huge quantity of Al in the wall structure of AlSBA-15.

Small-angle XRD pattern of Ni and Pt/AlSBA-15(5, 7 and 14) catalysts almost the same as pure AlSBA-15 supports, but the intensity of the reflection d_{100} characteristic diffraction peak became lower after Pt and Ni incorporation compared with bare AlSBA-15 samples. This probably due to strong X-ray absorption nature of Ni and Pt [146] or loss of long range order of mesostructure as a result of partial blocking of support pores by added Pt and Ni species.[147]

The length of the hexagonal unit cell a_o and d_{100} spacing of Ni and Pt-supported AlSBA-15 (5, 7 and 14) samples are shown in Table 6. The observed a_o values for the Ni and Pt-supported AlSBA-15 catalyst samples are found to be higher than the a_o value of the parent AlSBA-15 (5,7 and 14) providing that nickel and platinum ions were included within the alumino silicate frame work.[137] The a_o values increased as metal concentration increases. However the catalyst sample 2.5 wt% Ni/AlSBA-15 (14) whose a_o value was lower than that of the pure AlSBA-15(14) suggesting that nickel ions were present as an extra framework species.

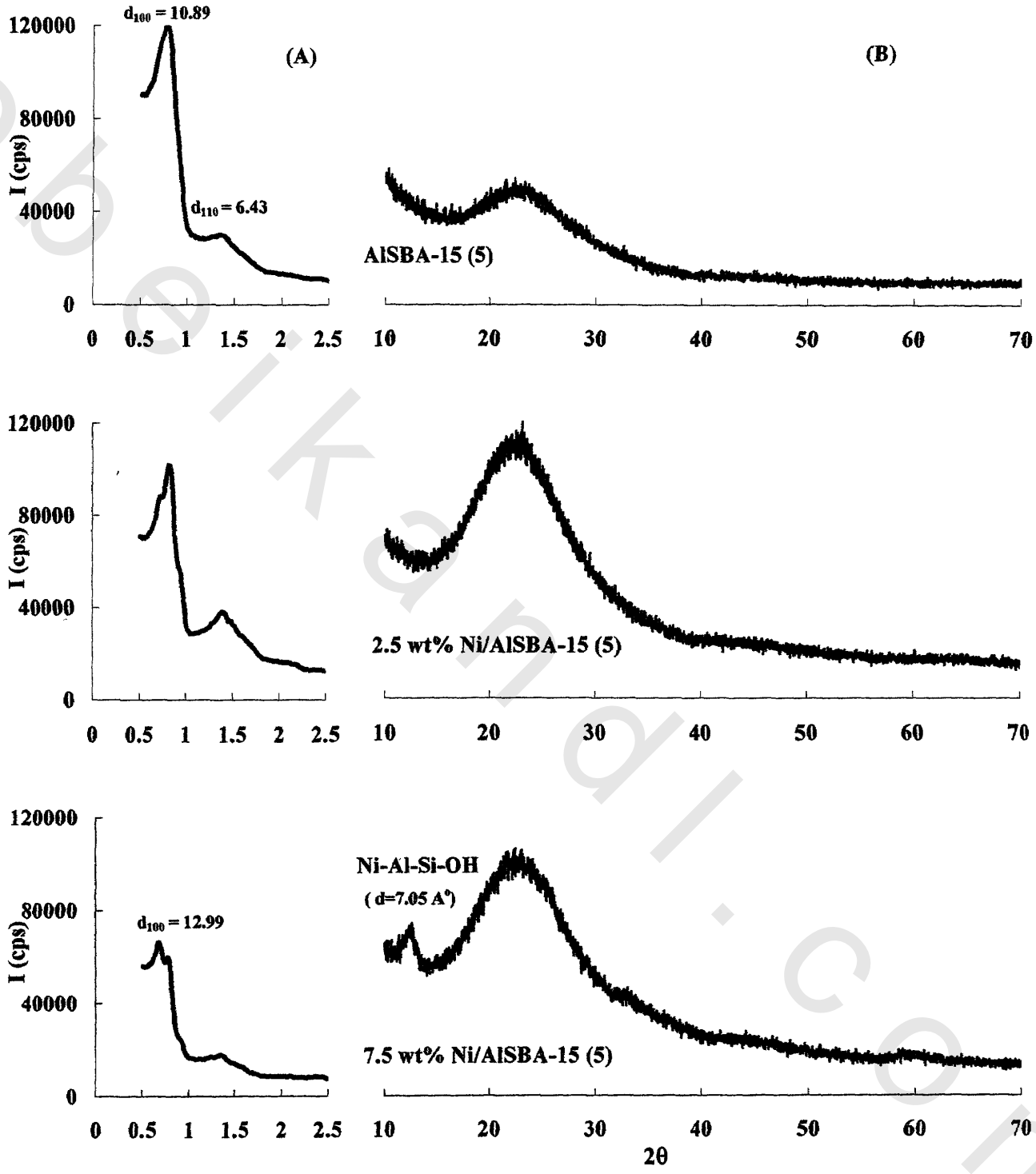

Fig. 20 (A) low angle XRD pattern and (B) wide angle XRD pattern of AlSBA-15(5) and Ni- supported catalysts

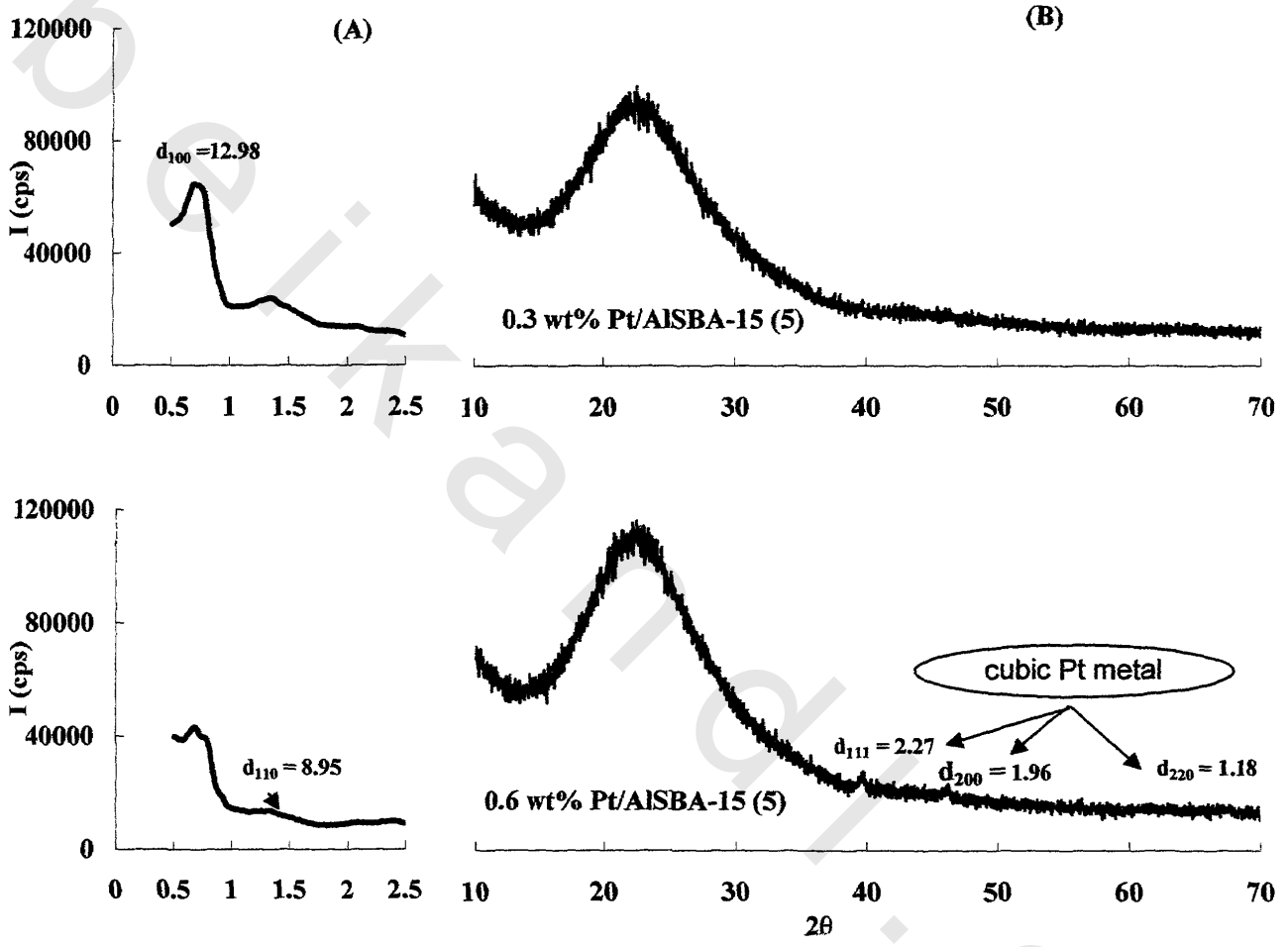

Fig.21 (A) low angle XRD pattern and (B) wide angle XRD pattern of Pt- supported AlSBA-15(5) catalysts

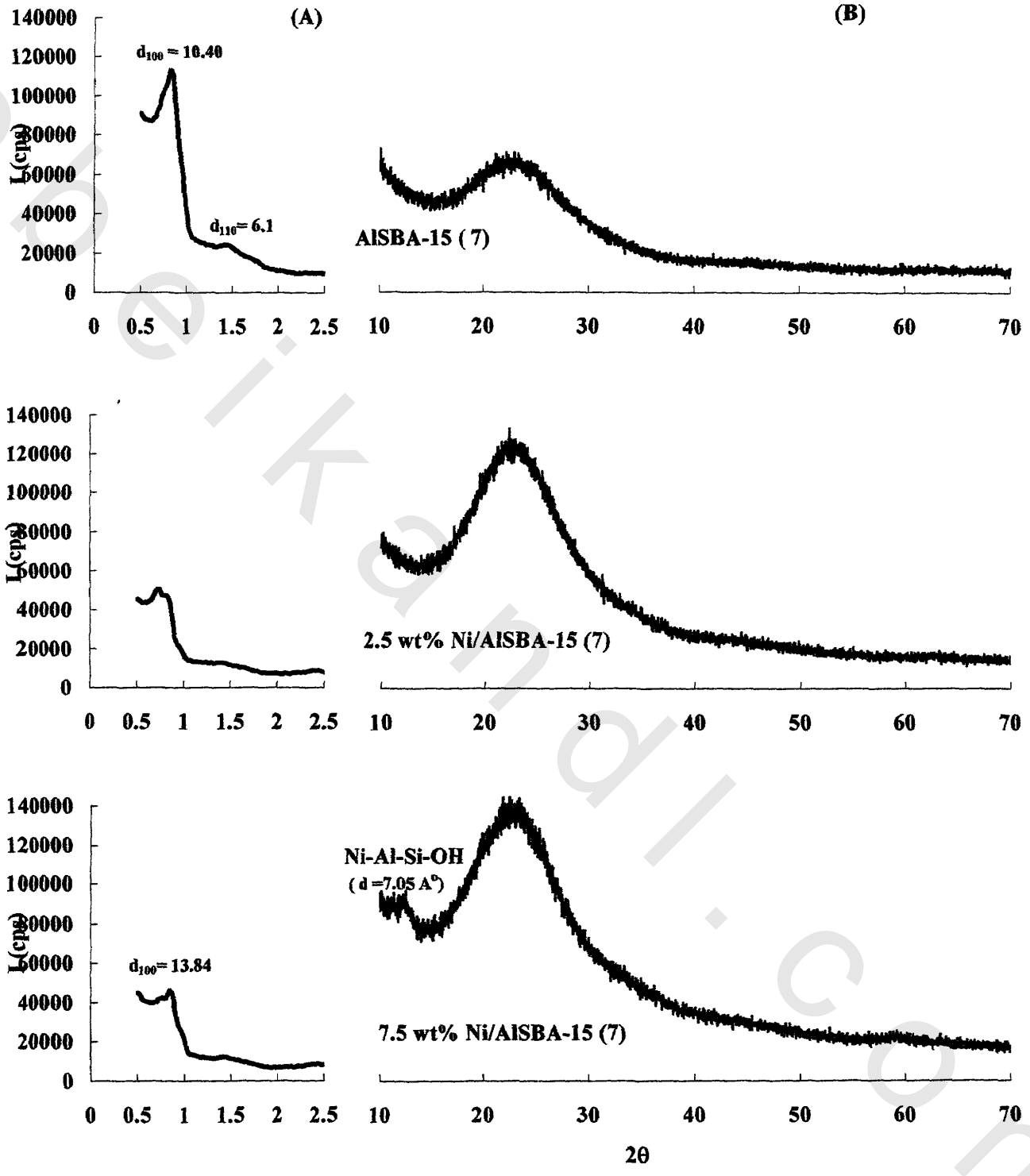

Fig.22 (A) low angle XRD pattern and (B) wide angle XRD pattern of AlSBA-15(7) and Ni- supported catalysts

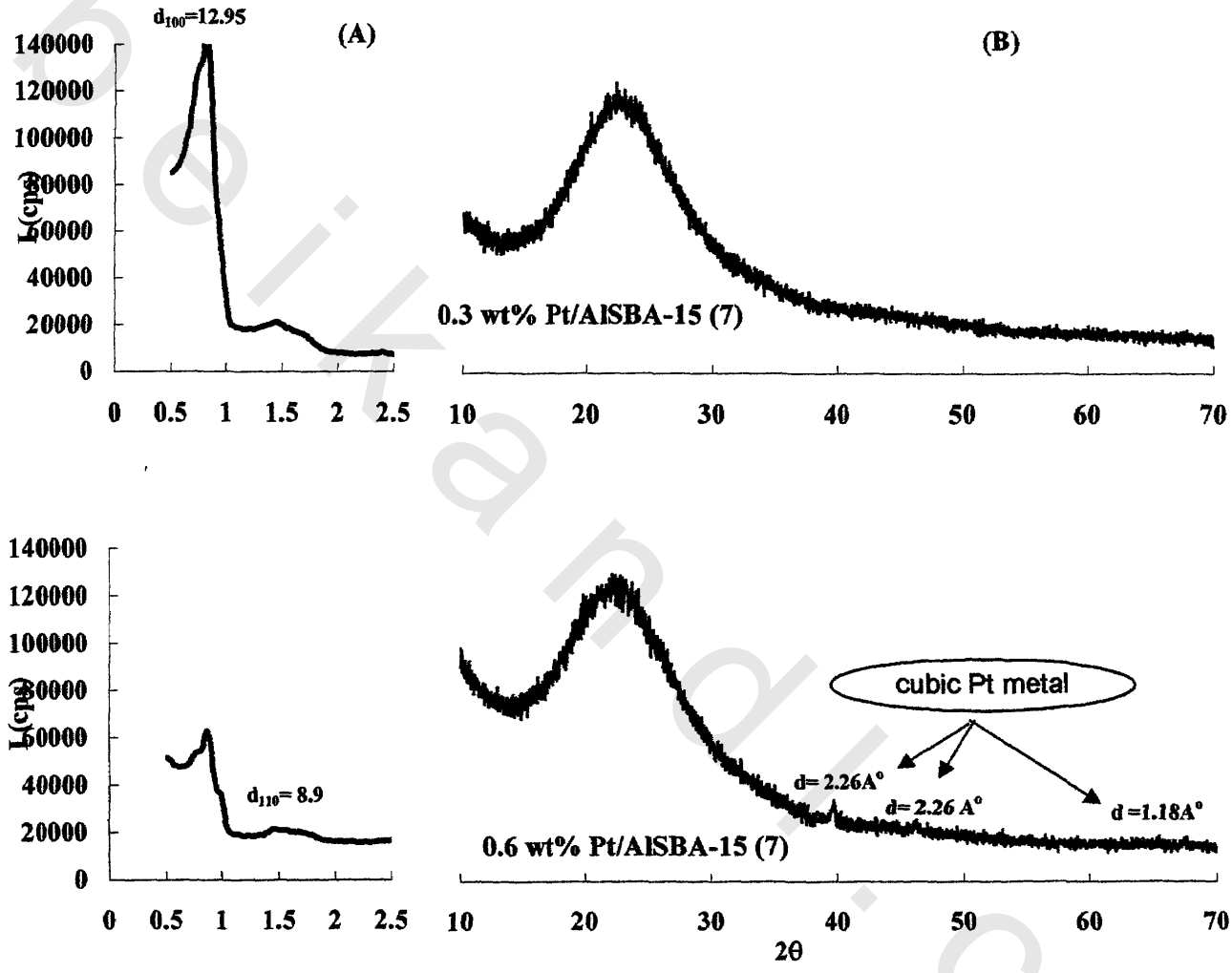

Fig.23 (A) low angle XRD pattern and (B) wide angle XRD pattern of Pt- supported AlSBA-15(7) catalysts

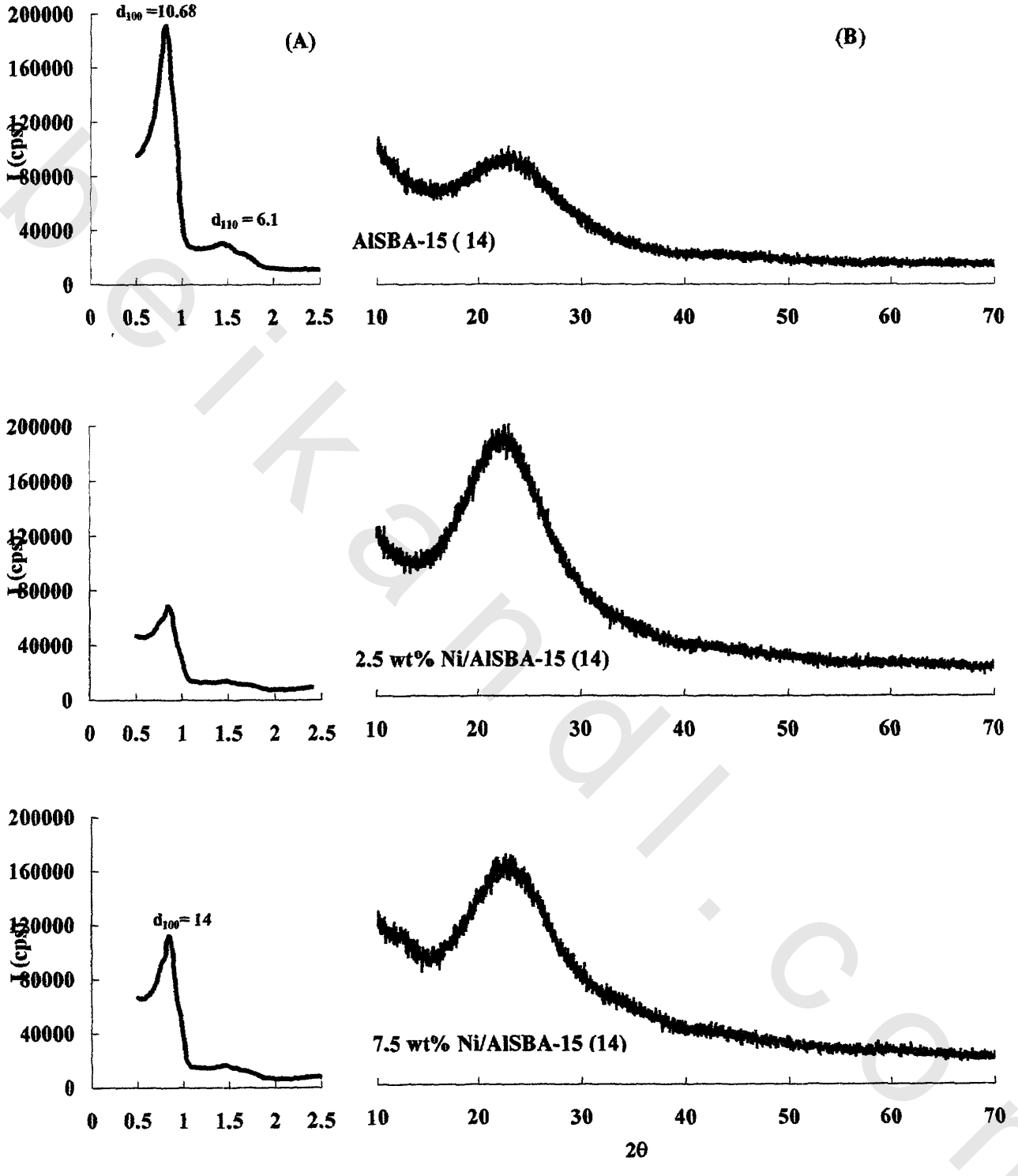

Fig.24 (A) low angle XRD pattern and (B) wide angle XRD pattern of AlSBA-15(14) and Ni- supported catalysts

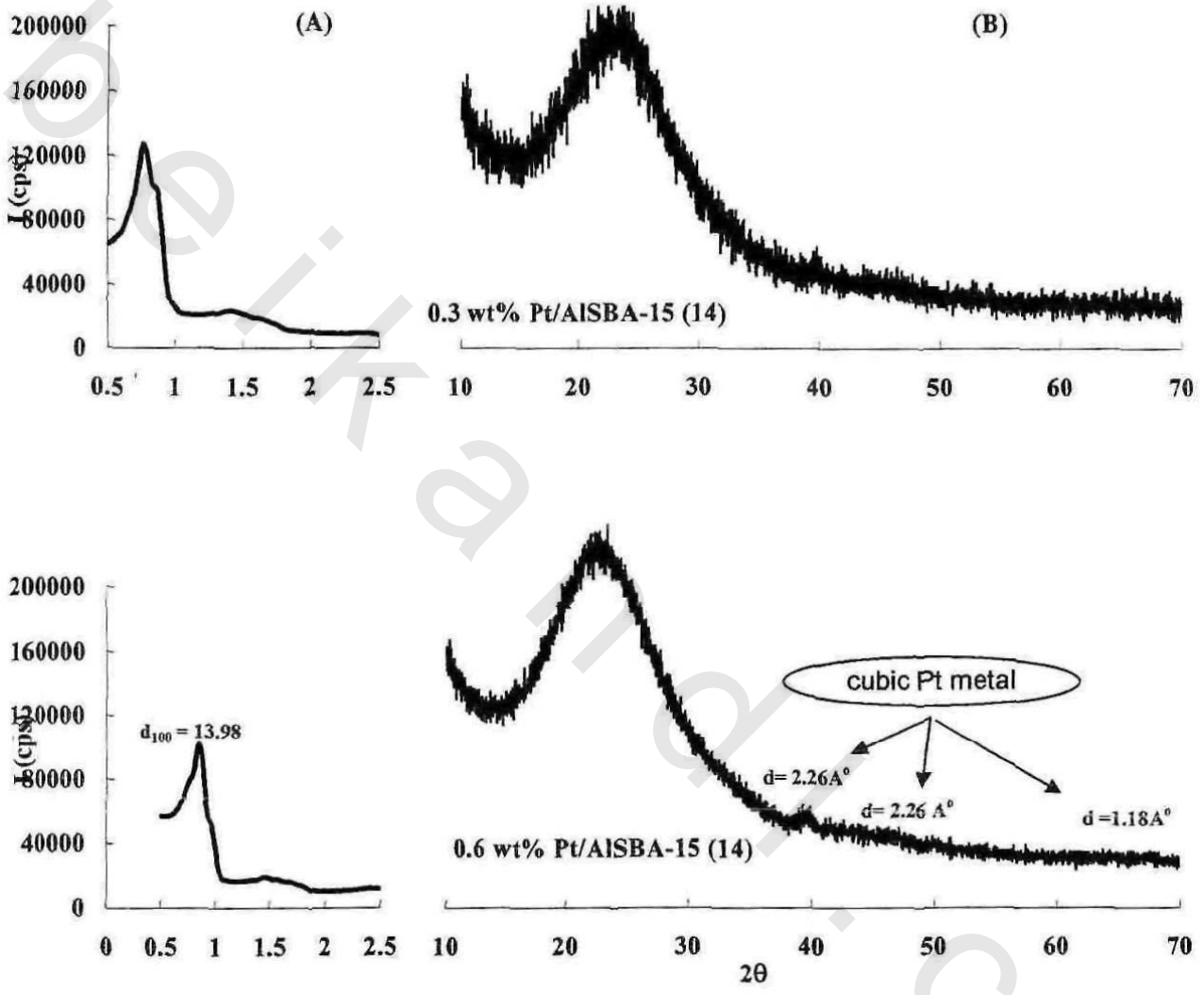

Fig.25 (A) low angle XRD pattern and (B) wide angle XRD pattern of Pt- supported AlSBA-15(14) catalysts

The pore wall thickness (T_{wall}) (Table 6) of Ni and Pt-supported catalysts was calculated based on the lattice cell parameter (a_o) and the pore diameter (P.D) ($T_{wall} = a_o$ - P.D), became thicker with respect to that of the purely AlSBA-15 (5, 7 and 14) materials and increased as the Pt and Ni concentration increases, indicating that nickel and platinum ions, are indeed, incorporated into the framework.

III.3. 2.1.2.Wide-angle XRD studies:

The wide-angle XRD patterns for Ni and Pt-supported AlSBA-15 (5, 7 and 14) catalyst samples in their oxidic state are shown in Figs. 20-25–B. All these samples showed the presence of broad reflection due to amorphous silica at $2\theta = 24^{o}$.

Powder XRD patterns for the catalyst sample containing 7.5wt% Ni (Figs.20,22 and 24-B), showed new crystalline species, similar to the standard pattern of nickel alumino silicate hydrate-like structure (Ni-Al-Si-OH) from the JCPDS powder diffraction file (PDF 26-1451) at d-spacing = 7.05Å. The formation of this phase resulted from the interaction of nickel oxide and aluminosilicates framework of the support. Thus the probability of Ni-Al-Si-OH crystal formation depends on the n_{Si}/n_{Al} ratio of the pure AlSBA-15 support, i.e. the peak intensity of this phase increases as the amount of aluminum in the support increases and as nickel concentration increases leading to formation of more Ni-Al-Si-OH crystals. This phase was not detected for catalyst sample 7.5 wt % Ni/AlSBA-15(14) which evidences a fine dispersion of Ni oxidic species on AlSBA-15(14) surface, either completely amorphous or composed of crystallites smaller than 4 nm.

The wide angle XRD patterns for Pt/AlSBA-15 (5, 7 and 14) were shown in Figs. 21, 23 and 25-B. They showed reflections at $2\theta = 39.7^{o}$, 46.2^{o} and 67.4^{o}, attributed to the cubic Platinum metal structure.[148] Their intensities increased with increasing Pt content (0.3-0.6 wt. % Pt).

Table 6: Textural parameters of AlSBA-15 (5,7 and 14), Ni and Pt-supported catalysts

Sample name	BET s.a ($m^2\ g^{-1}$)[a]	P.V ($mL\ g^{-1}$)[b]	P.D (nm)[c]	dV/dD[d]	2θ	$d_{(100)}$ (nm)[e]	a_o (nm)[f]	T_{wall} (nm)[g]
AlSBA-15 (5)*	**655**	**1.18**	**10.1**	**4.9**	**0.81**	**10.89**	**12.57**	**2.47**
2.5%NiO/AlSBA-15	603	1.08	8.1	4.5	0.68	12.95	14.95	7.05
7.5%NiO/AlSBA-15	464	0.63	7.9	3.5	0.67	12.99	15.00	6.90
0.3%PtO/AlSBA-15	734	1.32	10.1	0.04	0.67	12.98	14.99	4.89
0.6%PtO/AlSBA-15	645	1.15	10.2	0.04	0.67	12.99	14.99	4.79
AlSBA-15(7)*	**780**	**0.94**	**8.1**	**2.8**	**0.85**	**10.41**	**12.02**	**3.92**
2.5%NiO/AlSBA-15	733	0.897	8.1	2.4	0.68	12.94	14.94	6.84
7.5%NiO/AlSBA-15	538	0.71	8.2	0.02	0.64	13.84	15.98	**7.78**
0.3%PtO/AlSBA-15	755	0.91	10.1	2.7	0.68	12.95	14.95	4.85
0.6%PtO/AlSBA-15	759	0.91	10	2.7	0.68	12.95	14.95	4.95
AlSBA-15 (14)*	**787**	**1.02**	**10.1**	**3.3**	**0.83**	**10.68**	**12.34**	**2.24**
2.5%NiO/AlSBA-15	528	0.74	7.1	0.02	0.84	10.56	12.20	5.09
7.5%NiO/AlSBA-15	460	0.66	9.2	0.01	0.63	14.00	16.17	6.97
0.3%PtO/AlSBA-15	772	0.99	8.7	0.03	0.68	12.94	14.94	6.24
0.6%PtO/AlSBA-15	723	0.93	6.8	0.03	0.63	13.98	16.14	9.34

*: gel (n_{Si} / n_{Al})

a: Surface area calculated from BET equation.

b: Pore volume calculated from the adsorption branch of isotherm at P/Po ~ 0.98.

c: Pore diameter calculated from the adsorption branch of the isotherm according to BJH method.

d: Obtained from pore size distribution curve at the apex of the pattern.

e: d spacing from XRD.

f: Unit cell parameters calculated using formula $a_o = 2d_{100}/\sqrt{3}$.

g: wall thickness calculated from the difference between a_o and pore diameter.

III.2.2. Surface Characteristics

N_2 adsorption-desorption isotherms of AlSBA-15(5, 7 and 14), nickel and platinum supported catalysts (Figs.26-34-A) correspond, according to IUPAC, to a typical irreversible type IV isotherm with H1 hysteresis loop. All isotherms show a sharp steep at relative pressure of 0.65-0.9, which confirms the presence of large mesopores and characteristic of the capillary condensation inside uniform cylindrical pores.

The starting point of the hysteresis is slightly shifted to lower P/P° values when aluminum amount is increased, indicating that alumination decreases the surface area.

The N_2 adsorption– desorption isotherms of Ni and Pt catalysts supported on AlSBA-15 (5, 7 and 14) show the hysteresis loop similar to that of pure AlSBA- 15 materials (Figs.27, 28,30,31,33 and 34 -A), but a significant decrease in the amount of the adsorbed N_2 was observed after Ni and Pt impregnation while the shape of isotherms were almost unchanged after Ni and Pt deposition indicating the preservation of the support pore structure.

The pore size distribution calculated from the adsorption branch of the isotherms; show a narrow distribution of mesopores (Figs.26-34-B).

The textural properties of the AlSBA-15 samples synthesized with different n_{Si}/n_{Al} ratios, the platinum and nickel-supported catalysts as a function of n_{Si}/n_{Al} ratio of AlSBA-15 support are shown in Table 6.

The amount of aluminum in the pure AlSBA-15 materials has consequential impact on their BET specific surface area, it can be seen that the surface area values decrease in a linear manner with the decrease of n_{Si}/n_{Al} ratio of the support (Table 6), suggesting the presence of aluminum oxide species inside the mesoporous of AlSBA-15.

The surface area, total pore volume and average pore diameter values of the corresponding nickel and platinum-supported catalysts have suffered a decrease compared to the bare support (Table 6). This decrease is greater in so far as the amount of nickel and platinum present in the catalyst is higher. The incorporation of Ni and Pt provokes a blockage of the support porosity due to deposition of Ni and Pt oxide particles via wetness impregnation method.

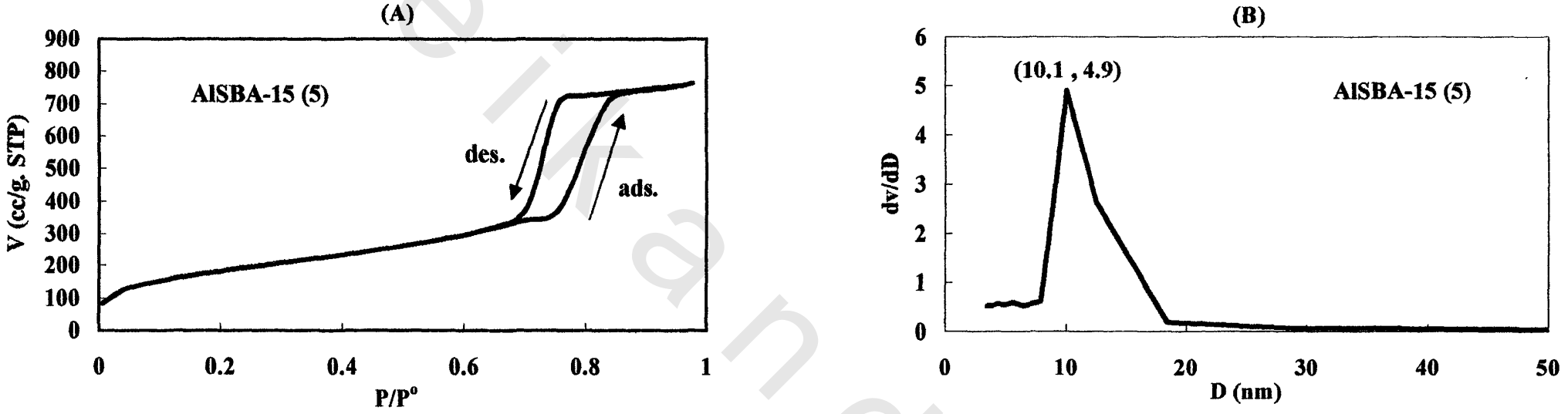

Fig.26 (A) the Nitrogen adsorption - desorption isotherm and (B) Pore Size Distrbution curve of Al SBA-15(5)

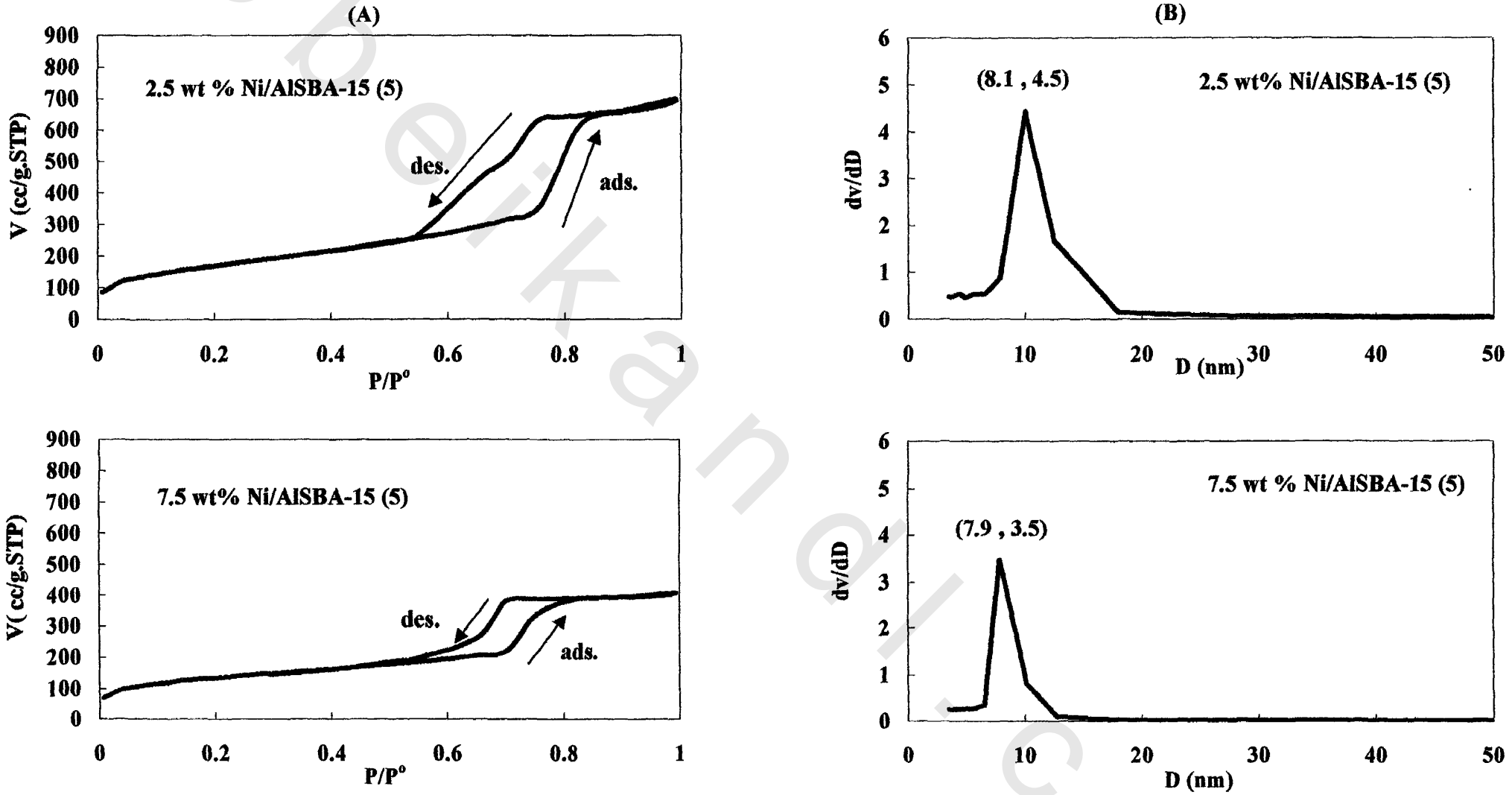

Fig. 27 (A) the Nitrogen adsorption - desorption isotherms and (B) Pore Size Distrbution curves of Ni/Al SBA-15(5) catalysts

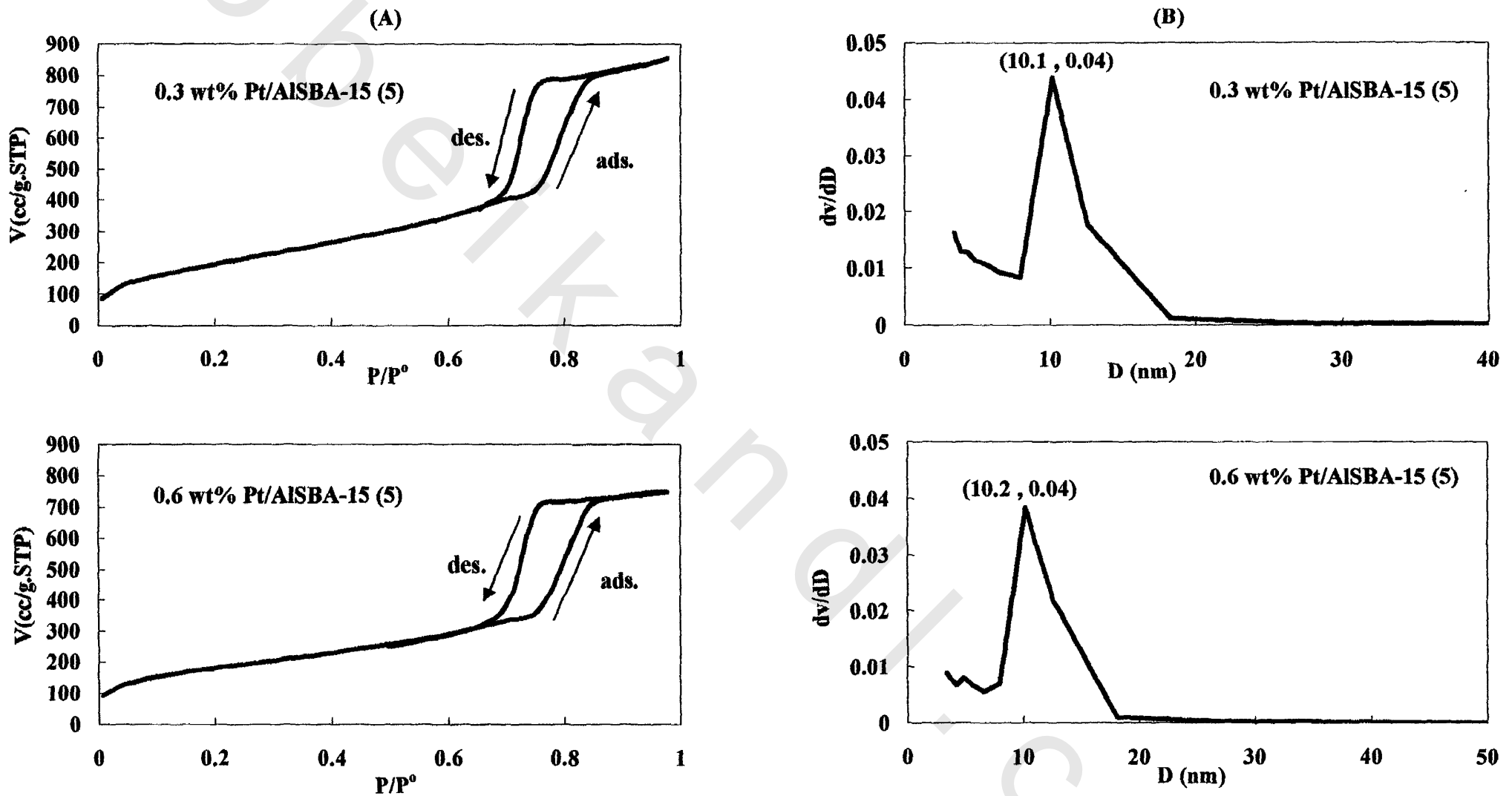

Fig.28 (A) the Nitrogen adsorption - desorption isotherms and (B) Pore Size Distrbution curves of Pt/Al SBA-15(5) catalysts

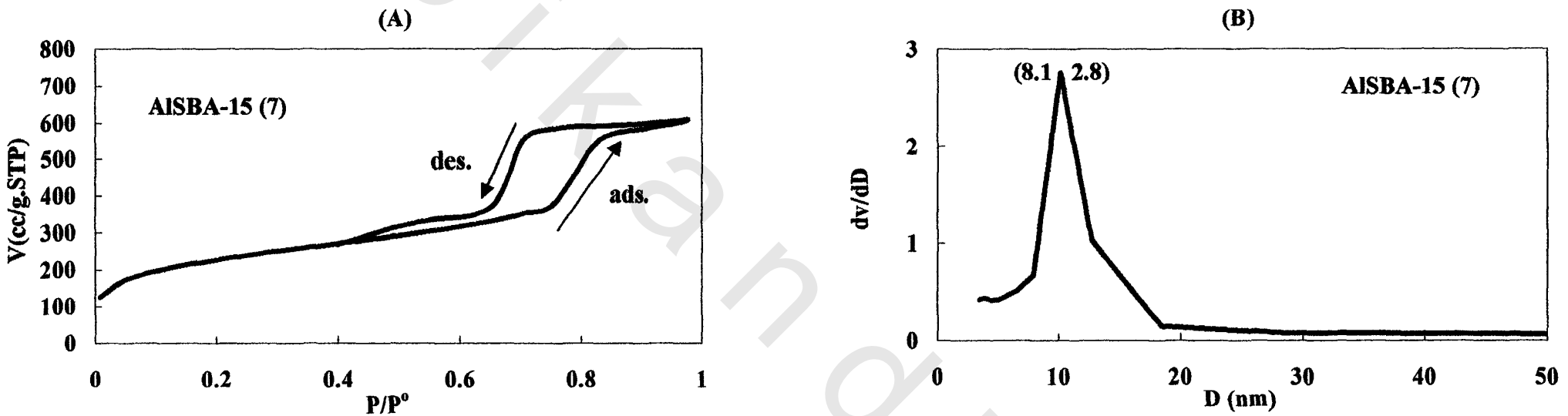

Fig.29 (A) the Nitrogen adsorption - desorption isotherm and (B) Pore Size Distrbution curve of Al SBA-15(7)

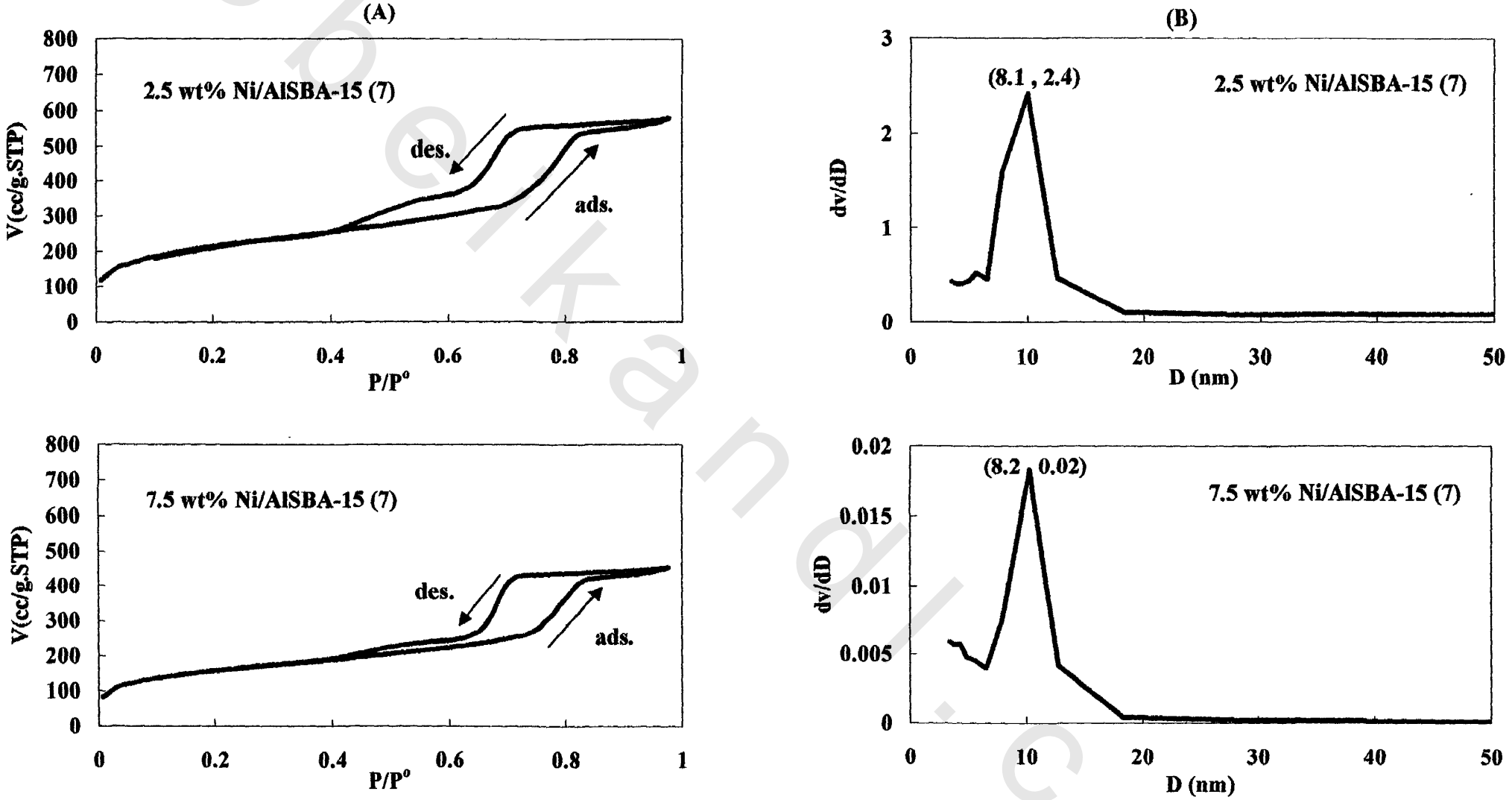

Fig.30 (A) the Nitrogen adsorption - desorption isotherms and (B) Pore Size Distrbution curves of Ni/Al SBA-15(7) catalysts

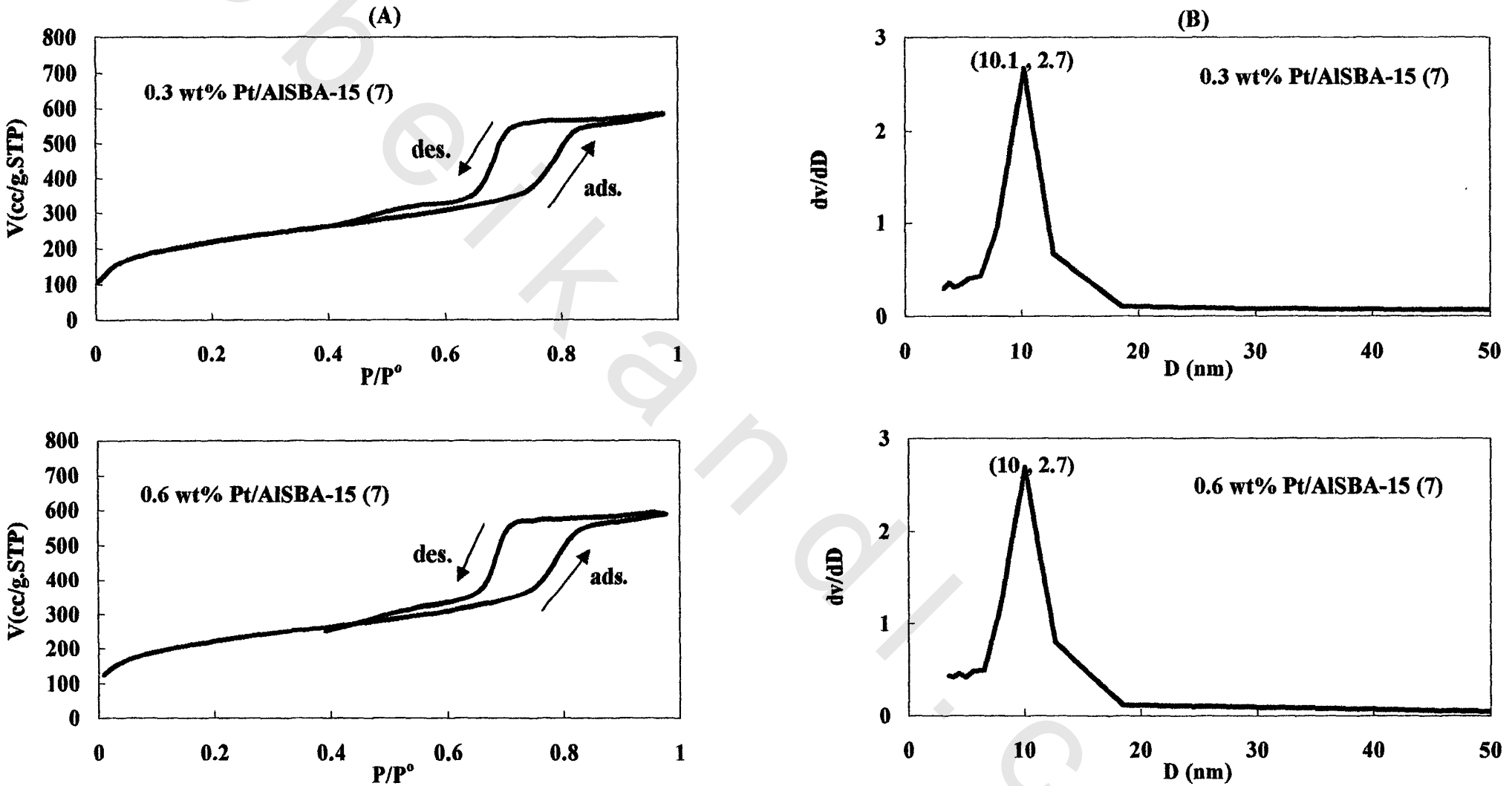

Fig.31 (A) the Nitrogen adsorption - desorption isotherms and (B) Pore Size Distrbution curves of Pt/Al SBA-15(7) catalysts

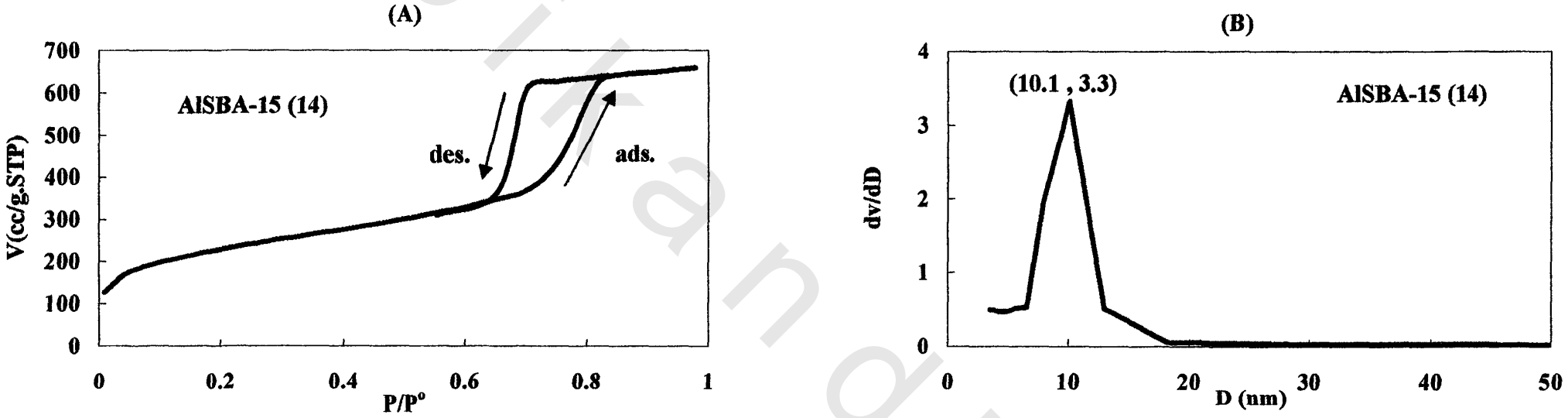

Fig. 32 (A) the Nitrogen adsorption - desorption isotherm and (B) Pore Size Distrbution curve of Al SBA-15(14)

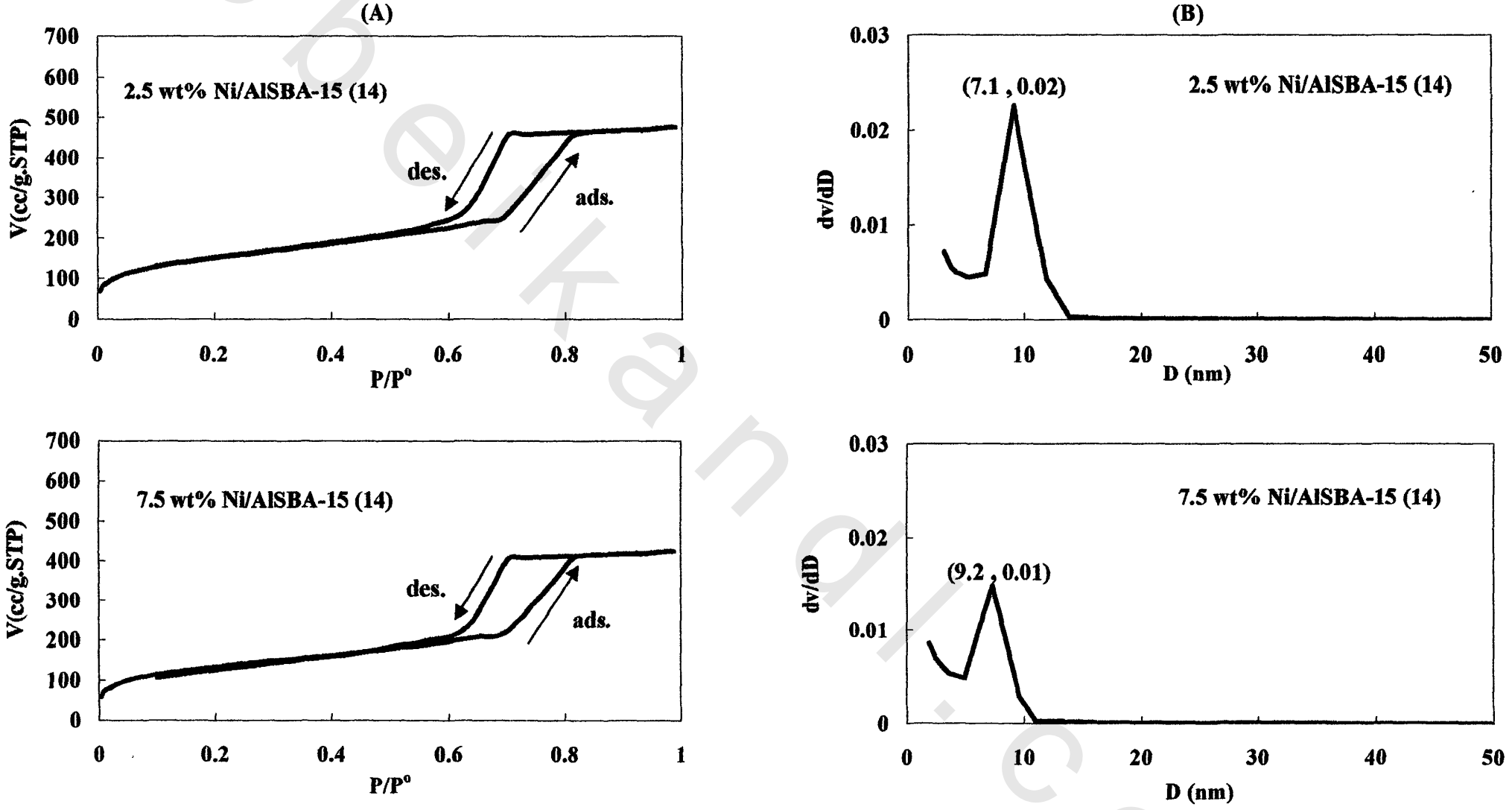

Fig. 33 (A) the Nitrogen adsorption - desorption isotherms and (B) Pore Size Distrbution curves of Ni/Al SBA-15(14) catalysts

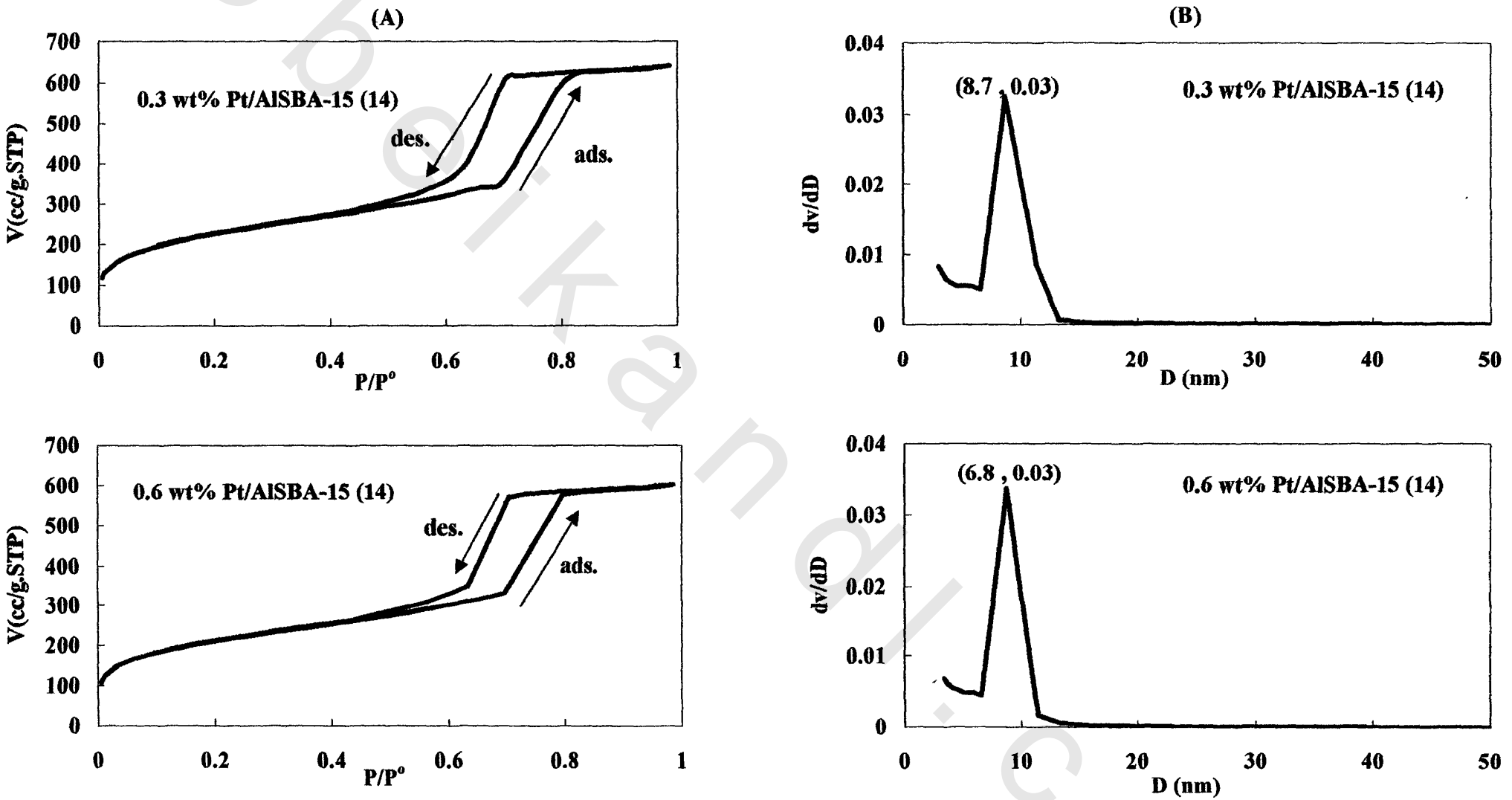

Fig. 34 (A) the Nitrogen adsorption - desorption isotherms and (B) Pore Size Distrbution curves of Pt/Al SBA-15(14) catalysts

The pore volume and average pore diameter values follow a similar trend. Except the catalyst sample 0.3 wt% Pt/AlSBA-15 (5) which had higher BET surface area (734) and pore volume (1.32) values if compared with pure AlSBA-15(5) while the pore diameter value maintained unchanged (10.1). In this catalyst sample happened penetration of Pt particles into the pores of bare AlSBA-15(5) support increasing its total pore volume. Consequently, the catalyst surface area increased with maintaining average pore diameter unchanged.

However, the textural properties of AlSBA-15 (5, 7 and 14) pure supports were more affected by Ni than Pt impregnation (Table 6).

Interestingly, the average pore diameter values increased for catalyst samples 0.3wt %Pt/AlSBA-15(7) and 0.6wt% Pt/ALSBA-15(7) (Table 6) accompanied by a decrease in their specific surface areas and the total pore volume indicating that some micropores were preferably blocked by metal particle, and the apparent average pore size of AlSBA-15 (7) increased with metal loading.[123]

III.2.3.Thermal Analysis

Pure supports, namely, AlSBA-15 (5), AlSBA-15 (7) and AlSBA-15 (14) (Figs.35-40 and Table 7) show one broad endothermic peak at $T_{max.}$ = 92, 75 and 83°C, respectively. This event is accompanied by weight loss as detected by TGA. The intensity and temperature of these endothermic peaks differed according to the n_{Si}/n_{Al} ratio of the support. This endothermic peak is attributed to the dehydration of the physisorbed water.

ΔH of the dehydration of physisorbed water event (Table 7) of the pure supports are increased as n_{Si}/n_{Al} ratio increases. This means that the dehydration of the physisorbed water process become more difficult with increasing n_{Si}/n_{Al} due to formation of strong hydrogen bonding between physisorbed water and excess free (OH) groups of the support. The excess free (OH) groups were related to the n_{Si}/n_{Al} ratio. The higher the n_{Si}/n_{Al} ratio was, the more excess free (OH) groups present in the support. This also accompanied by the increase in weight loss as n_{Si}/n_{Al} ratio increased as detected by TGA which attributed to the more physisorbed water molecules desorbed from the pure support.

III.2.3.1. Nickel loaded over AlSBA-15 with different n_{Si}/n_{Al} ratios

By loading AlSBA-15(5, 7 and14) with 2.5 and 7.5 wt%Ni (Figs.35, 37 and 39-A) and Table 7, a broad endothermic peak was observed at $T_{max.}$ = 83-90 °C. This peak corresponds to the dehydration of the physisorbed water. This event is accompanied by weight loss as detected by TGA (Figs.35, 37 and 39-B) and Table 7. ΔH and ΔS for this event increased (34 -75cal. /g) as nickel loading increased. This is attributed to the increase of nickel oxide on the surface of the support.

Another endothermic peak was observed at $T_{max.}$ = 300, 260 and 320 °C (Table 7). Its intensity becomes more pronounced with nickel loading and accompanied with weight loss as detected by TGA (Figs.35, 37 and 39-B) and Table 7. This event corresponds to the dehydroxylation of OH present in Ni-Al-Si-OH phase resulting from metal-support interaction. This is also in harmony with XRD results.

Generally, the dehydroxylation process of OH from Ni-Al-Si-OH phases (Second event) is easier than the dehydration process (first event) of physisorbed water according to the ΔH, Cp and ΔS values of both processes (Table 7).

III.2.3.2. Platinum loaded over AlSBA-15 with different n_{Si}/n_{Al} ratios

Figs. 36, 38 and 40-A represent the DSC curves of supported Pt catalysts. These curves have one endothermic peak corresponding to the dehydration of the surface physisorbed water. The shallow and broad endothermic events were observed at $T_{max.}$ = 75-87 °C. This event is accompanied by weight loss as detected by TGA (Figs. 36, 38 and 40-B) and Table 7.

For all Pt supported catalysts, both ΔH and ΔS of the dehydration event (Table 7) increases compared with those of the pure supports. This is due the coverage of the adsorption sites of the support by platinum particles thus the dehydration process becomes difficult and endothermic peak is broadened. But the ΔH and weight loss values were almost the same for samples contained 0.3 and 0.6 wt% Pt.

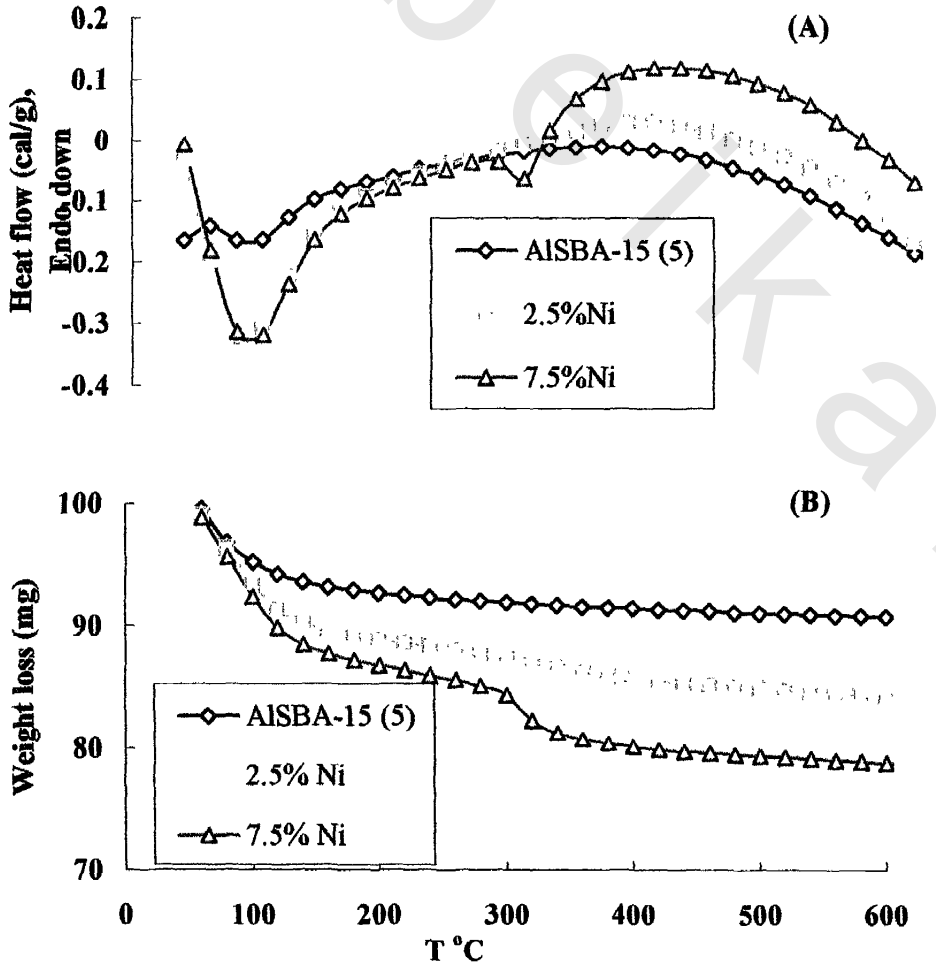

Fig.35 (A) DSC and (B) TGA curvesof AlSBA-15(5) and Ni /AlSBA-15(5)

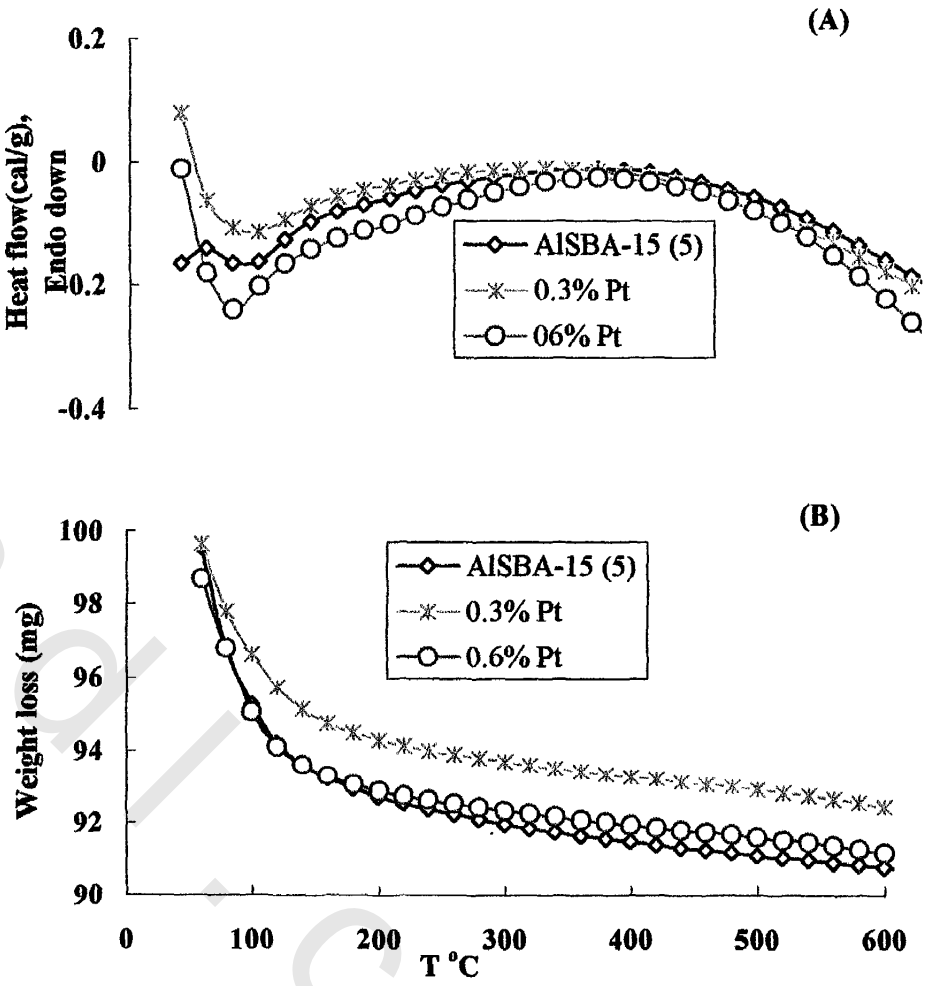

Fig. 36 (A) DSC and (B) TGA curves of AlSBA-15(5) and Pt /AlSBA-15(5)

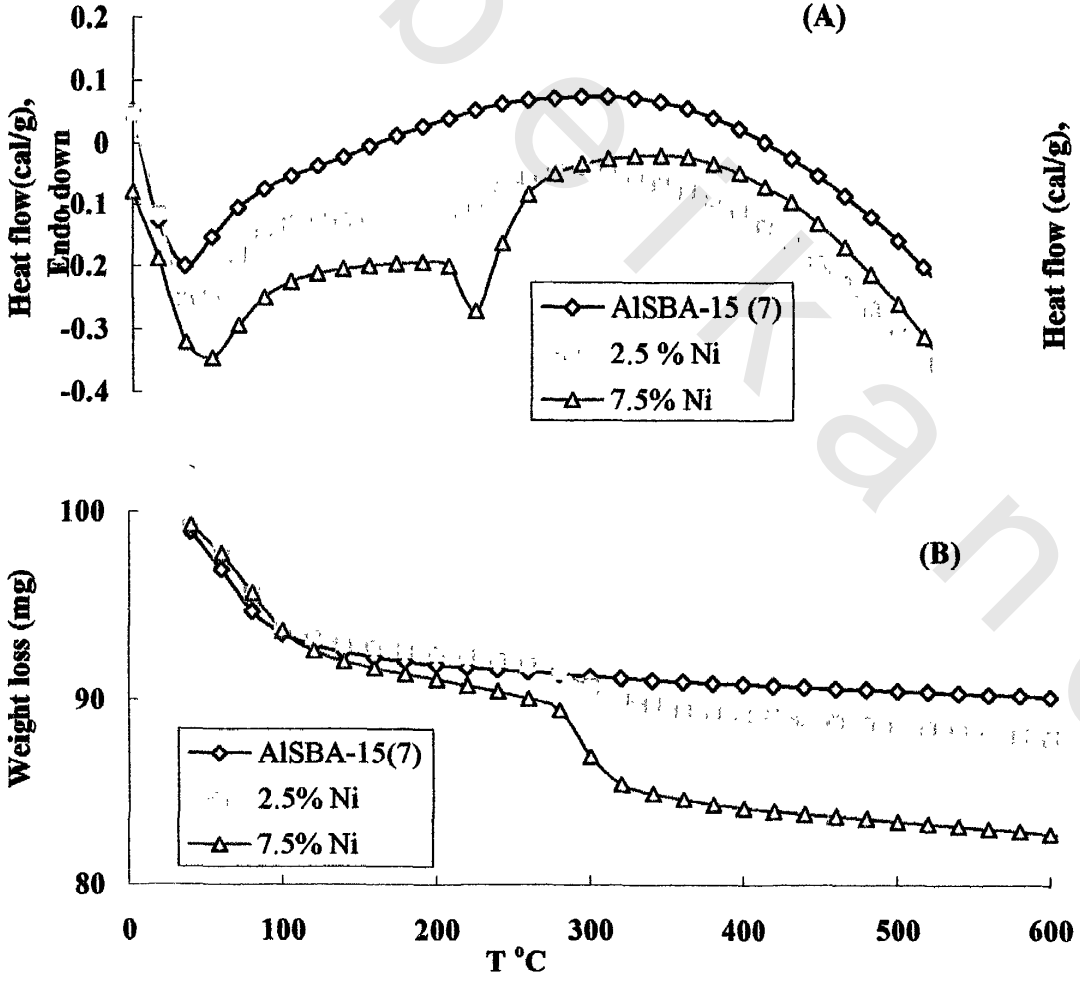

Fig. 37 (A) DSC and (B) TGA curves of AlSBA-15(7) and Ni /AlSBA-15(7)

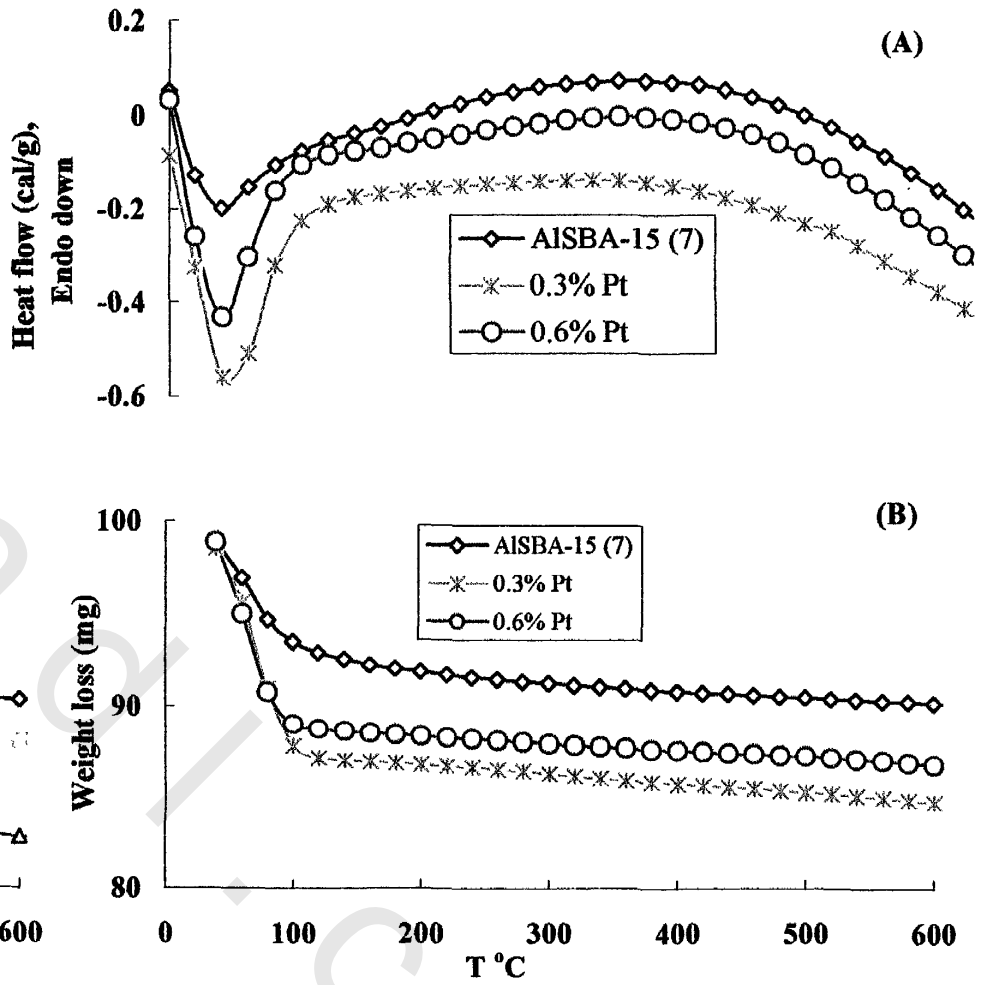

Fig. 38 (A) DSC (B) TGA curves of AlSBA-15(7) and Pt /AlSBA-15(7)

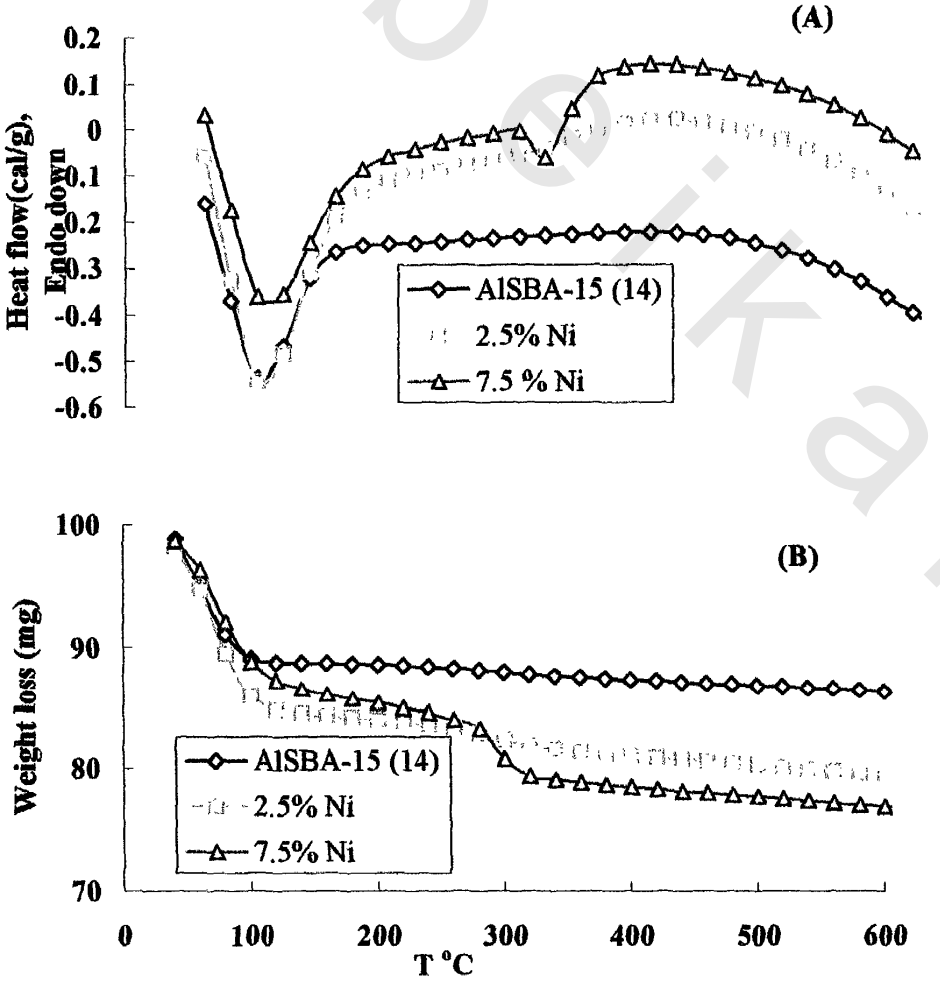

Fig. 39 (A) DSC and (B) TGA curves of AlSBA-15(14) and Ni /AlSBA-15(14)

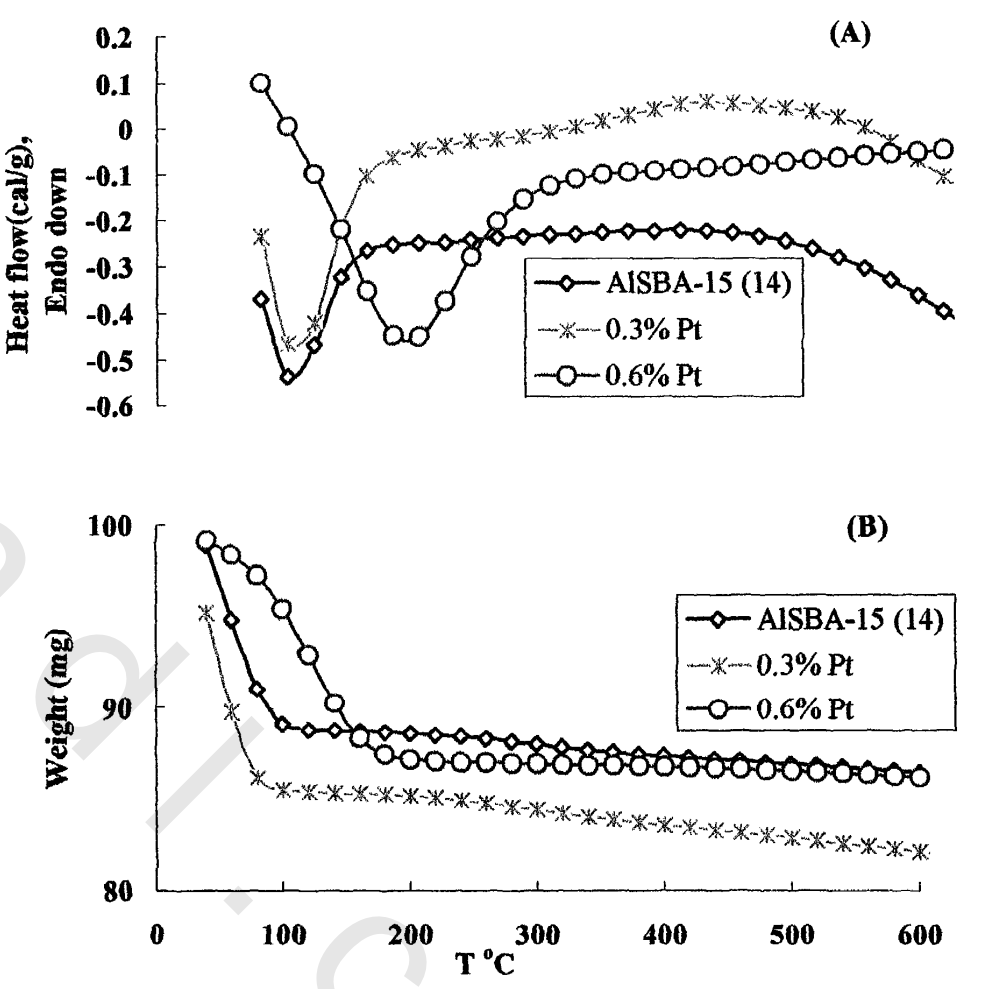

Fig.40 (A) DSC and (B) TGAcurves of AlSBA-15(14) and Pt /AlSBA-15(14)

Table 7: DSC and TGA of AlSBA-15(5, 7 and14), Ni and Pt-supported AlSBA-15 catalysts

Sample name	1st event							2nd event						
	T_1 (°C)	T_2 (°C)	$T_{max.}$ (°C)	ΔH (Cal/g.)	wt loss (mg)	Cp (Cal/g . deg)	ΔS (Cal/g . deg)	T_1 (°C)	T_2 (°C)	$T_{max.}$ (°C)	ΔH (Cal/g)	wt loss (mg)	Cp (Cal/g . deg)	ΔS (Cal/g . deg)
AlSBA-15 (5)	62	128	92	5	0.31	0.08	0.06	-	-	-	-	-	-	-
2.5%Ni	46	136	85	34	0.63	0.38	0.41	-	-	-	-	0.18	-	-
7.5%Ni	36	146	86	54	0.77	0.49	0.69	260	320	300	8	0.31	0.13	0.03
0.3%Pt	44	146	85	21	0.37	0.21	0.25	-	-	-	-	-	-	-
0.6%Pt	49	113	75	13	0.30	0.2	0.17	-	-	-	-	-	-	
AlSBA-15 (7)	45	130	75	25	0.43	0.29	0.31	-	-	-	-	-	-	-
2.5%Ni	33	137	83	33	0.44	0.32	0.46	220	300	260	1	0.11	0.01	0.003
7.5%Ni	52	141	90	36	0.45	0.4	0.4	240	300	260	10	0.33	0.17	0.04
0.3%Pt	49	135	86	71	0.88	0.83	0.84	-	-	-	-	-	-	-
0.6%Pt	34	124	78	67	0.8	0.74	0.96	-	-	-	-	-	-	-
AlSBA-15 (14)	41	136	83	48	0.75	0.51	0.61	-	-	-	-	-	-	-
2.5%Ni	44	142	84	69	0.92	0.7	0.82	280	360	320	2	0.14	0.03	0.008
7.5%Ni	38	152	85	75	0.92	0.66	0.92	300	360	320	8	0.29	0.13	0.02
0.3%Pt	45	145	87	68	0.89	0.68	0.8	-	-	-	-	-	-	-
0.6%Pt	42	135	84	63	0.81	0.68	0.79	-	-	-	-	-	-	-

DSC curves of Pt/AlSBA-15 (5, 7 and 14) catalysts don't show a second endothermic peak (dehydroxylation event) as in case of Ni/AlSBA-15 (5, 7 and 14) catalysts. This is attributed to the fact Pt don't interact with hydroxyl groups present in supports (The main phase is Pt).

III.2.4.Catalytic Activity

The catalytic activity of the prepared catalysts, namely, 0.3 and 0.6 wt%Pt/AlSBA-15(5, 7 and 14), 2.5 and 7.5 wt%Ni/AlSBA-15(5, 7 and 14) were tested through Cyclohexane dehydrogenation and n-hexane hydroconversion (hydroisomerization and hydrocarcking). This part deals with the effect of the metals, their concentration and the n_{Si}/n_{Al} ratio of AlSBA-15 support on the catalytic processes.

III.2.4.1. Catalytic activity of Pt/AlSBA-15(5) catalysts

(A) Cyclohexane conversion

Cyclohexane dehydrogenation over 0.3 and 0.6 wt%Pt/AlSBA-15 to benzene increased by temperature increasing in the range 250-450°C and decreases by platinum concentration (Figs.41 and 42-A) and Table 8.

The yield (mole %) of benzene increases sharply with the temperature for the catalyst containing 0.3 wt% Pt achieving 100% in the temperature range (300-450 °C), while as, it increases gradually for the sample containing 0.6 wt% achieving 100% in the temperature range (350- 450 °C).No sign of formation of cracking products of cyclohexane under the operating conditions. The dehydrogenation of cyclohexane into benzene selectivity is 100% over the whole range of temperature, (250-450 °C).

The dehydrogenation activity of the catalyst sample containing 0.3 wt% Pt/AlSBA-15(5) is higher than that of 0.6 wt%Pt/AlSBA-15(5).this may be due to Pt dispersion over the surface of the support.

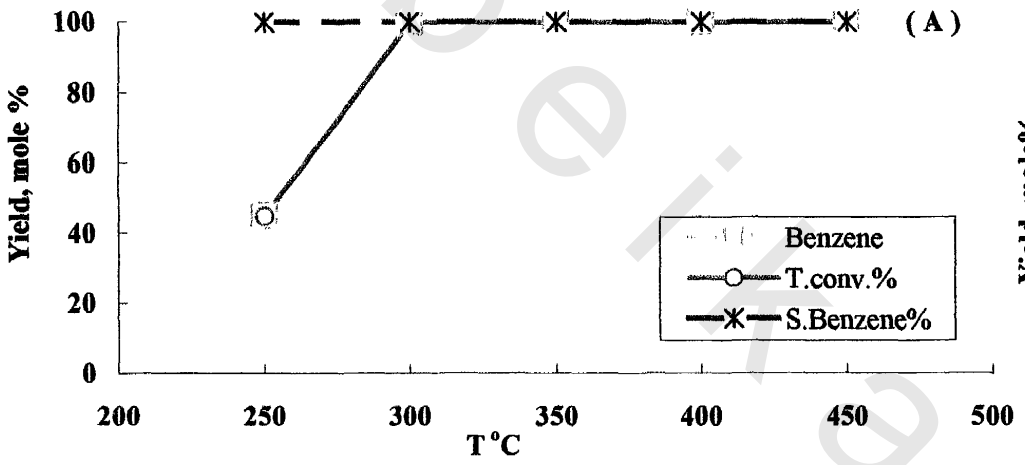

Fig. 41 The catalytic conversion of (A) cyclohexane (B) n-hexane over 0.3 wt% Pt/AlSBA-15(5)

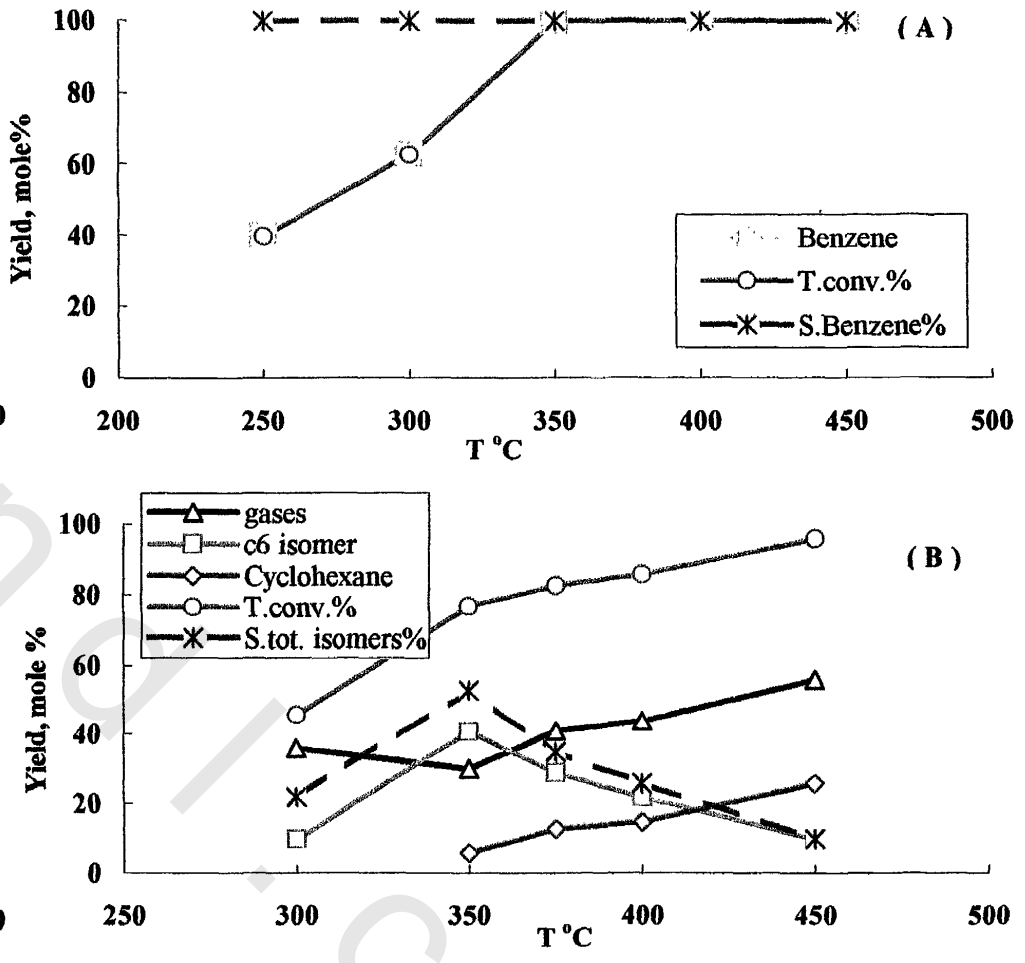

Fig. 42 The catalytic conversion of (A) cyclohexane (B) n-hexane over 0.6 wt%Pt/AlSBA-15 (5)

Table 8: Catalytic conversion of cyclohexane over Pt /AlSBA-15 (5) catalysts: (A) 0.3 wt%Pt and (B) 0.6 wt%Pt

Reaction products	Reaction temperature, °C				
	250	300	350	400	450
(A) Benzene	45	100	100	100	100
Cyclohexane	70	55	0	0	0
T.Conv. %	30	45	100	100	100
S.Benzene%	100	100	100	100	100
(B) Benzene	40	63	100	100	100
Cyclohexane	60	37	0	0	0
T.Conv. %	40	63	100	100	100
S.Benzene%	100	100	100	100	100

Table 9: Catalytic conversion of n-hexane over Pt /AlSBA-15 (5) catalysts: (A) 0.3 wt%Pt and (B) 0.6 wt%Pt

Reaction products	Reaction temperature, °C					
	300	325	350	375	400	450
(A) gases	9	20	17	24	37	55
C_6 isomer	16	32	37	30	24	19
C_6	75	48	31	25	24	14
Mecyclopentane	0	0	8	7	0	0
Cyclohexane	0	0	7	14	15	12
T.Conv. %	25	52	69	75	76	86
S. tot. isomers%	64	62	65	49	32	22
(B) gases	36	31	30	41	49	60
C_6 isomer	10	13	35	29	22	10
C_6	54	46	23	17	14	4
Mecyclopentane	0	4	6	0	0	0
Cyclohexane	0	6	6	13	15	26
T.Conv. %	46	54	77	83	86	96
S. tot. isomers%	22	31	53	35	26	10

(B) n-hexane conversion

The catalytic conversion of n-hexane over Pt/AlSBA-15 with different Pt loading (Viz., 0.3 and 0.6 wt% pt) catalysts (Figs. 41 and 42-B) and Table 9, give rise to different Reactions: cracking (gases), isomerization (C_6- isomers + methyl cyclopentane) and cyclization (cyclohexane). All the reactions start at temperature ≥ 300 °C. The isomerization Activity of 0.3 wt%Pt/AlSBA-15 was higher than 0.6 wt% Pt/AlSBA-15. The yield (mole %) of total isomers (C_6- isomers + methyl cyclopentane) at 350 °C is 45% for the catalyst sample containing 0.3 wt% Pt but relatively lower (41%) for sample containing 0.6 wt% Pt. the total conversion and mole% of cyclohexane increased by increasing the reaction temperature and Pt concentration.

On the contrary, the gas yield increases from 9-55% (at 300- 450 °C) and 36-60% (at 300-450 °C) for samples containing 0.3 and 0.6 wt% Pt, respectively.

The isomerization selectivity decreases with both reaction temperature and Platinum concentration (Figs.41 and 42-B).

III.2.4.2. Catalytic activity of Ni/AlSBA-15 (5) catalysts

(A)Cyclohexane conversion

Cyclohexane dehydrogenation to benzene increases over Ni/AlSBA-15 catalysts with different nickel loading 2.5 and 7.5 wt% Ni shown in Figs. 43 and 44-A and Table 10.

The yield (mole%) of benzene increases with temperature reaching maximum at 300 °C and then declines due to appearance of gaseous cracking products. At 300 °C, the mole% of benzene increases by nickel loading for the sample containing 7.5wt% Ni (28%) and 2.5 wt% Ni (25%).The sample containing 2.5wt% Ni is more active one toward benzene formation than the sample containing 7.5wt% Ni. The cyclohexane cracking (propane formation) increases by both temperature and nickel loading, at the expense of benzene formation. Cyclohexane cracking started at lower temperature for higher nickel loading and increases as nickel loading decreases.

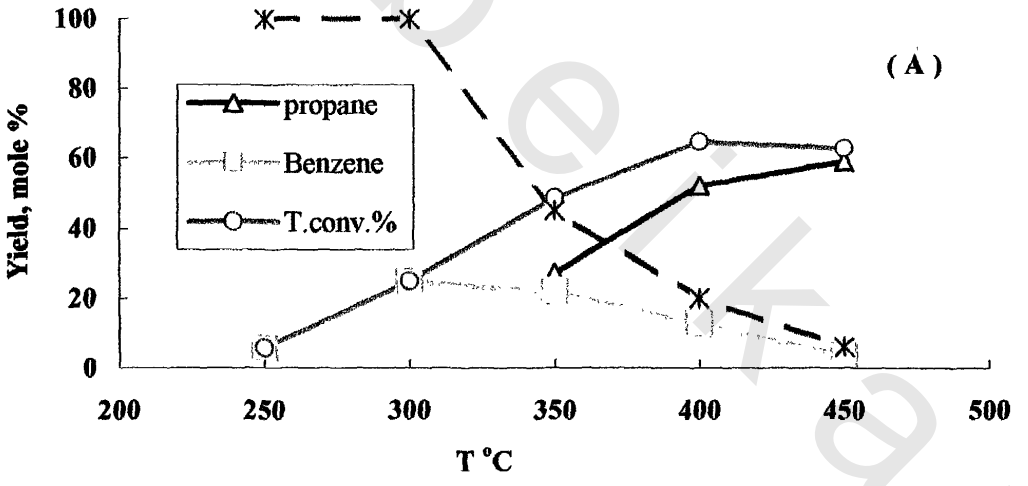

Fig.43 The catalytic conversion of (A) cyclohexane (B) n-hexane over 2.5 wt% Ni / AlSBA-15 (5)

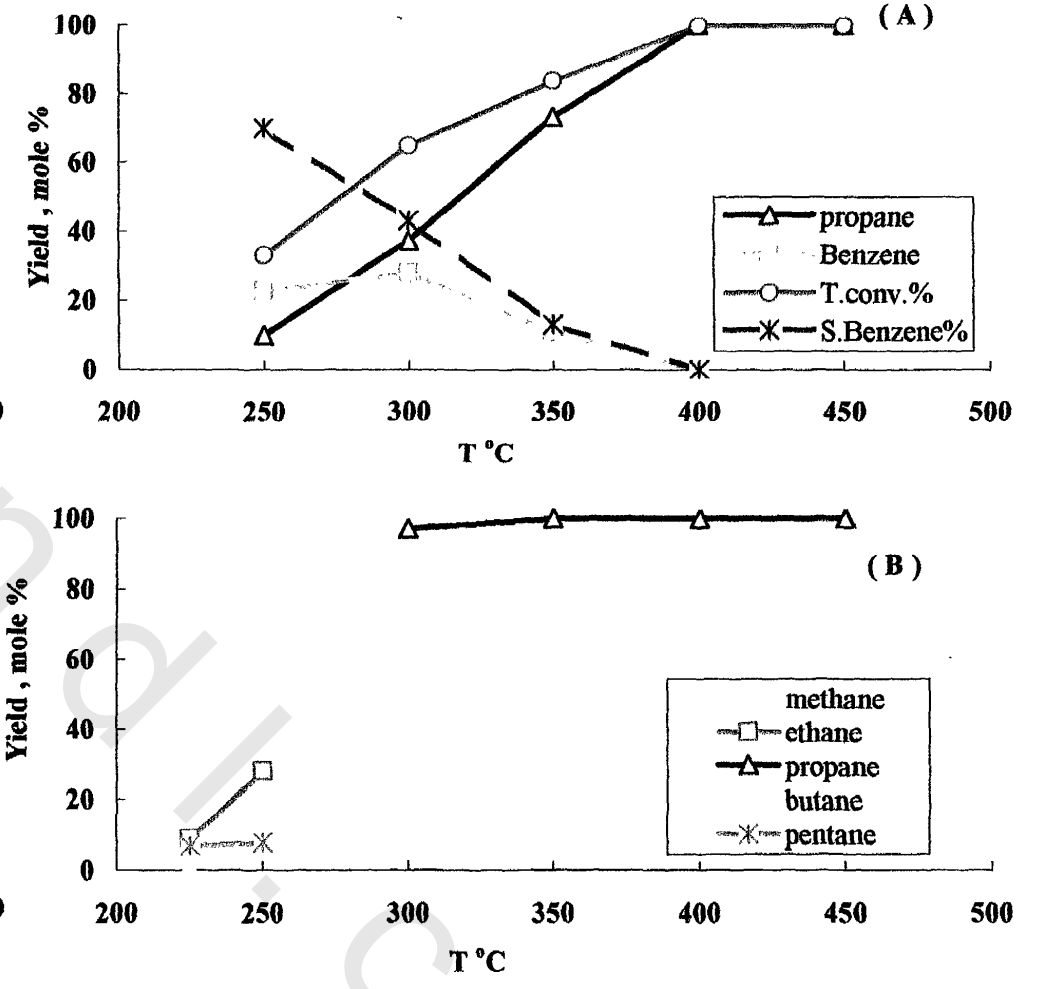

Fig.44 The catalytic conversion of (A) cyclohexane (B) n-hexane over 7.5 wt% Ni/AlSBA-15(5)

Table 10: Catalytic conversion of cyclohexane over Ni /AlSBA-15 (5) catalysts: (A) 2.5 wt%Ni and (B) 7.5 wt%Ni

Reaction products	Reaction temperature, °C				
	250	300	350	400	450
(A) propane	0	0	27	52	59
Benzene	6	25	22	13	4
Cyclohexane	94	75	51	35	37
T.Conv. %	6	25	49	65	63
S.Benzene%	100	100	45	20	6
(B) propane	10	37	73	100	100
Benzene	23	28	11	0	0
Cyclohexane	67	35	16	0	0
T.Conv. %	33	65	84	100	100
S.Benzene%	70	43	13	0	0

Table 11: Catalytic conversion of n-hexane over Ni /AlSBA-15 (5) catalysts: (A) 2.5 wt%Ni and (B) 7.5 wt%Ni

Reaction products	Reaction temperature, °C				
	250	300	350	400	450
(A) methane	8	21	0	0	0
ethane	12	22	0	0	0
propane	0	0	64	79	80
butane	6	11	0	0	0
pentane	18	5	0	0	0
n-hexane	56	41	36	21	20
(B) methane	34	0	0	0	0
ethane	28	0	0	0	0
propane	0	97	100	100	100
butane	15	0	0	0	0
pentane	8	0	0	0	0
n-hexane	15	3	0	0	0

The total conversion on catalyst sample containing 2.5 wt% Ni is higher than that on 7.5 wt% Ni referring to benzene formation rather than cracking products (Figs. 43 and 44-A).

(B) n-hexane conversion

n- hexane cracking into propane is the most dominating reaction over Ni/AlSBA-15 catalysts with different nickel loading 2.5 and 7.5 wt% Ni (Figs.43 and 44-B) and Table 11.

The yield (mole %) of propane increases as reaction temperature and nickel loading increases. At 350 °C, the mole % of propane increases by nickel loading. The propane yield reaches 64% and 100% at 350 °C for catalyst sample containing 2.5 and 7.5wt% Ni, respectively. Beside propane formation, methane, ethane, butane and pentane are formed as cracking side products (at 225-250 °C for sample containing 7.5 wt%Ni) and (at 250-300 °C for sample containing 2.5 wt%Ni).The yield of each reaction is quantitatively small and increases slightly by temperature and nickel loading (Figs. 43 and 44 -B).

III.2.4.3. Catalytic activity of Pt/AlSBA-15 (7) catalysts

(A) Cyclohexane conversion

Cyclohexane dehydrogenation over Pt/AlSBA-15 to benzene and the total conversion increase by temperature and platinum loading (0.3-0.6 wt%Pt) in the range, (250-450 °C) (Figs.45 and 46-A) and Table 12.

Benzene mole % increases sharply for the catalyst containing 0.6wt%Pt achieving 100% at 300 °C, while as, it increases gradually with the temperature for the catalyst containing 0.3 wt% Pt achieving its maximum value of 100% at 350 °C and then declines due to appearance of propane as gaseous cracking product especially at higher temperature (above 350 °C). The selectivity of benzene formation reaches the maximum value of 100% over the temperature range (250-350 °C) and then decreases due to appearance of propane as side product for both Pt loading, Figs. 45 and 46-A.

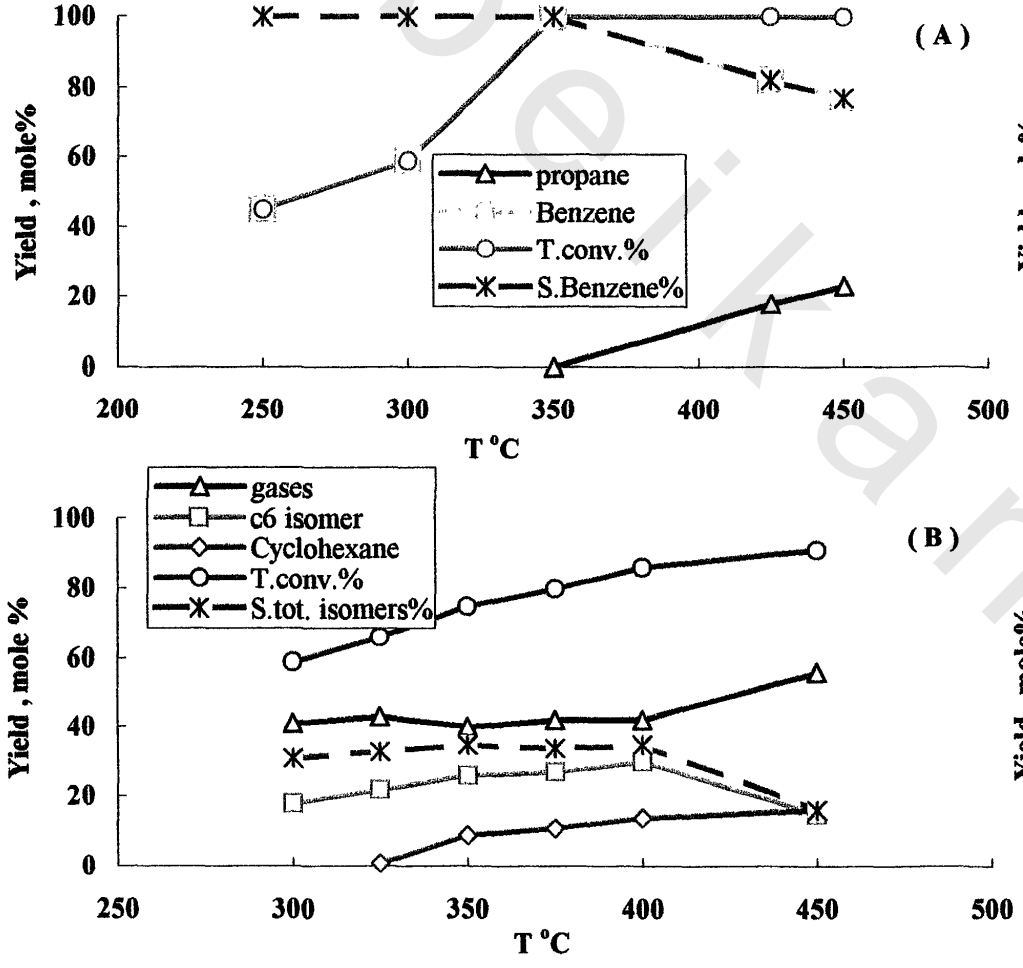

Fig. 45 The catalytic conversion of (A) cyclohexane (B) n-hexane over 0.3 wt% Pt/AlSBA-15(7)

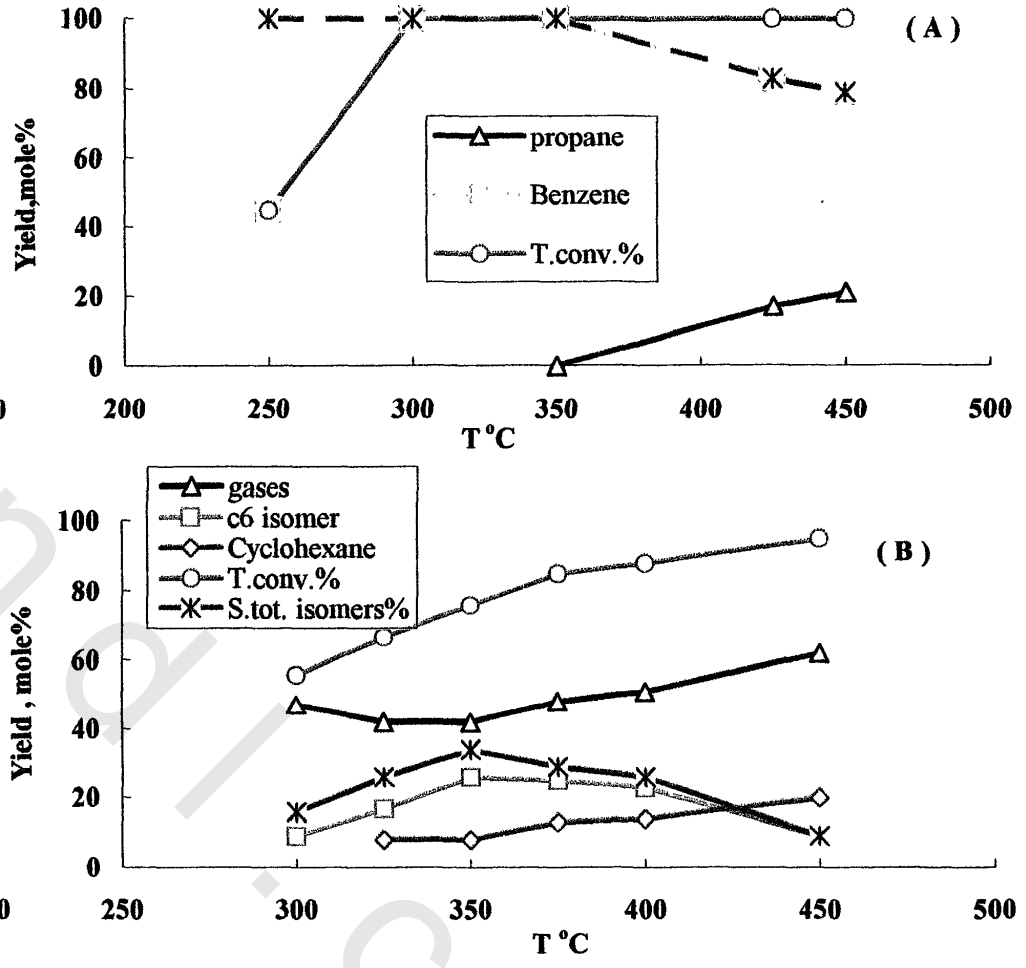

Fig. 46 The catalytic conversion of (A) cyclohexane (B) n-hexane over 0.6 wt% Pt/AlSBA-15(7)

Table 12: Catalytic conversion of cyclohexane over Pt /AlSBA-15 (7) catalysts: (A) 0.3 wt%Pt and (B) 0.6 wt%Pt

Reaction products	Reaction temperature, °C				
	250	300	350	425	450
(A) propane	0	0	0	18	23
Benzene	45	59	100	82	77
Cyclohexane	55	41	0	0	0
T.Conv. %	45	59	100	100	100
S.Benzene%	100	100	100	82	77
(B) propane	0	0	0	17	21
Benzene	45	100	100	83	79
Cyclohexane	55	0	0	0	0
T.Conv. %	45	100	100	100	100
S.Benzene%	100	100	100	83	79

Table 13: Catalytic conversion of n-hexane over Pt /AlSBA-15 (7) catalysts: (A) 0.3 wt%Pt and (B) 0.6 wt%Pt

Reaction products	Reaction temperature, °C					
	300	325	350	375	400	450
(A) gases	41	43	40	42	42	56
C_6 isomer	9	14	18	21	30	15
C_6	41	34	25	20	14	9
Mecyclopentane	9	8	8	6	0	0
Cyclohexane	0	1	9	11	14	16
T.Conv. %	59	66	75	80	86	91
S. tot. isomers%	31	33	35	34	35	16
(B) gases	47	42	42	48	51	62
C_6 isomer	9	17	14	25	23	9
C_6	44	33	24	14	12	5
Mecyclopentane	0	0	8	0	0	0
Cyclohexane	0	8	8	13	14	20
T.Conv. %	56	67	76	86	88	95
S. tot. isomers%	16	26	34	29	26	9

(B) n-hexane conversion

Catalyst sample containing 0.3 wt% Pt/AlSBA-15 has the higher activity towards n-hexane isomerization (Figs.45 and 46-B and Table 13) than the catalyst sample containing 0.6 wt% Pt/AlSBA-15 although they gave approximately equal amounts of isomers. The total isomers (C_6- isomers + methyl cyclopentane) are higher and steady in value for the whole temperature (300-450 °C) in case of sample containing 0.3 wt%Pt (Table 13). Beside isomer products, cracking gases and cyclohexane are formed. The mole % of gases and cyclohexane increased with both reaction temperature and platinum concentration. The isomerization selectivity decreases with both reaction temperature and platinum concentration (Figs.45 and 46 -B).

III.2.4.4.Catalytic activity of Ni/AlSBA-15 (7) catalysts

(A) Cyclohexane conversion

Cyclohexane dehydrogenation to benzene increases steadily for sample containing 2.5 wt% Ni by increasing temperature reaching a maximum of 39% at 300 °C and then declines, (Figs.47 and 48-A) and Table 14 while as, for the sample containing 7.5wt%Ni, cyclohexane dehydrogenation decreases by temperature increasing from (250-450 °C), Figs. 47 and 48-A) and Table 14.

The catalyst sample containing 2.5 wt% Ni/AlSBA-15 is more active one towards benzene formation than 7.5 wt% Ni/AlSBA-15.

Beside benzene formation, propane is formed by cyclohexane cracking and its yield increases by increasing temperature and nickel loading (Figs. 47and 48 -A).

(B) n-hexane conversion

The catalytic conversion of n-hexane over Ni/AlSBA-15 catalysts with different Ni loading (2.5 and 7.5 wt% Ni) was shown in Figs. 47 and 48 -B and Table15.

Cracking of n-hexane into propane increases by temperature and nickel loading. At 350 °C, the mole % of propane reaches 81 % and 96 % for catalyst sample containing 2.5wt% Ni/AlSBA-15 and 7.5wt% Ni/AlSBA-15, respectively.

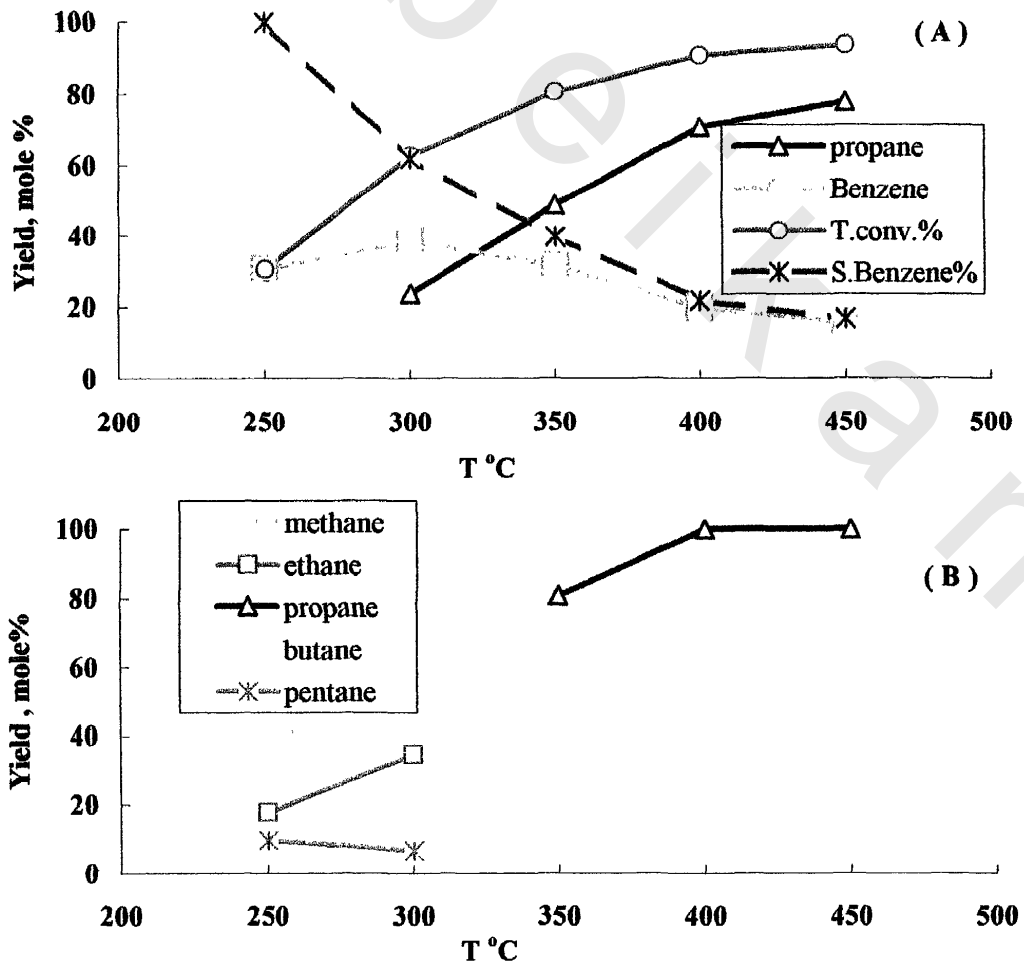

Fig. 47 The catalytic conversion of (A) cyclohexane (B) n-hexane over 2.5 wt % Ni/AlSBA-15 (7)

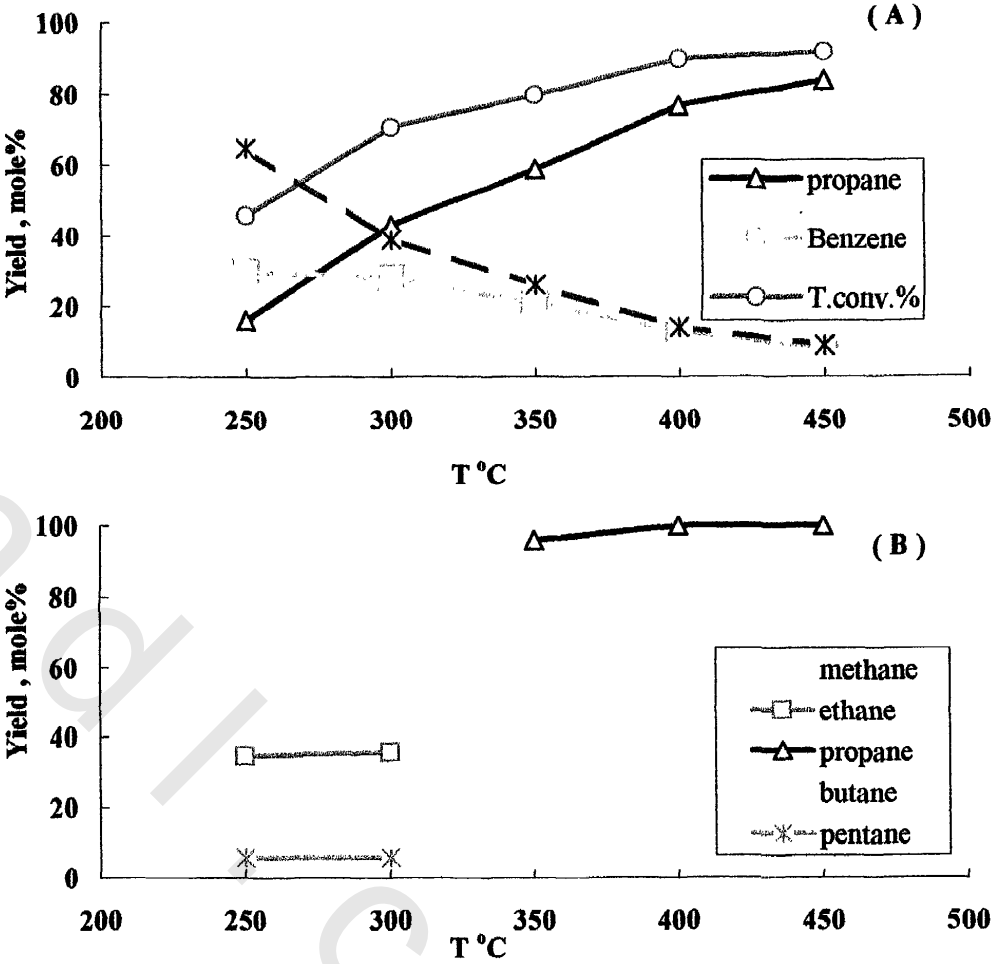

Fig. 48 The catalytic conversion of (A) cyclohexane (B) n-hexane over 7.5 wt % Ni/AlSBA-15 (7)

Table 14: Catalytic conversion of cyclohexane over Ni /AlSBA-15 (7) catalysts: (A) 2.5 wt%Ni and (B) 7.5 wt%Ni

Reaction products	Reaction temperature, °C				
	250	300	350	400	450
(A) propane	0	24	49	71	78
Benzene	31	39	32	20	16
Cyclohexane	69	37	19	9	6
T.Conv. %	31	63	81	91	94
S.Benzene%	100	62	40	22	17
(B) Propane	16	43	59	77	84
Benzene	30	28	21	13	8
Cyclohexane	54	29	20	10	8
T.Conv. %	46	71	80	90	92
S.Benzene%	65	39	26	14	9

Table 15: Catalytic conversion of n-hexane over Ni /AlSBA-15 (7) catalysts: (A) 2.5 wt%Ni and (B) 7.5 wt%Ni

Reaction products	Reaction temperature, °C				
	250	300	350	400	450
(A) methane	44	32	0	0	0
ethane	18	35	0	0	0
propane	0	0	81	100	100
butane	9	18	0	0	0
pentane	10	7	0	0	0
n-hexane	19	8	19	0	0
(B) methane	27	26	0	0	0
ethane	35	36	0	0	0
propane	0	0	96	100	100
butane	18	19	0	0	0
pentane	6	6	0	0	0
n-hexane	14	13	4	0	0

At lower temperature ≤ 300 °C many cracking products such as (methane, ethane, butane and pentane) are formed as side products. The yield of each product increases by reaction temperature and Ni loading (Figs. 47 and 48-B).

III.2.4.5. Catalytic activity of Pt/AlSBA-15 (14) catalysts

(A) Cyclohexane conversion

Catalytic dehydrogenation of cyclohexane over Pt/AlSBA-15 catalyst samples containing 0.3 and 0.6 wt%Pt were represented in Figs. 49 and 50-A and Table 16 reveals that, the total conversion increases by increasing the reaction temperature in the range 250-450 °C and decreases with increasing Pt loading .

For the catalyst sample containing 0.3 wt% Pt/AlSBA-15, the mole% of benzene sharply increases with temperature reaching a constant maximum value of ~ 100% over the temperature range (350-450 °C). No sign of presence of cracking side reaction under the operating conditions and thus the selectivity of benzene formation, reaches maximum value at 100% over the whole temperature range. While as, for the catalyst sample containing 0.6 wt % Pt/AlSBA-15 the yield of benzene increases sharply with temperature reaching 100% maximum value at 350 °C then decreases due to appearance of propane as a result of cyclohexane cracking at higher temperature (above 400 °C). Consequently, the selectivity of benzene formation decreases by increasing the temperature. The sample 0.3 wt % Pt is the active one towards cyclohexane dehydrogenation into benzene if compared with 0.6 wt % Pt sample.

(B) n-hexane conversion

The catalytic conversion behavior of n-hexane over Pt/AlSBA-15 is approximately the same as Pt/AlSBA-15 (5 and 7) catalyst samples in the whole temperature range (250-450 °C) as shown in Figs. 49 and 50-B and Table 17. The isomerization activity in this case is proportional to platinum concentration. The total isomers (C_6- isomers + methyl cyclopentane) at 375 °C are 16% for the sample containing 0.3 wt% Pt, but relatively higher 24% for the sample containing 0.6 wt%Pt. The isomerization selectivity decreases with

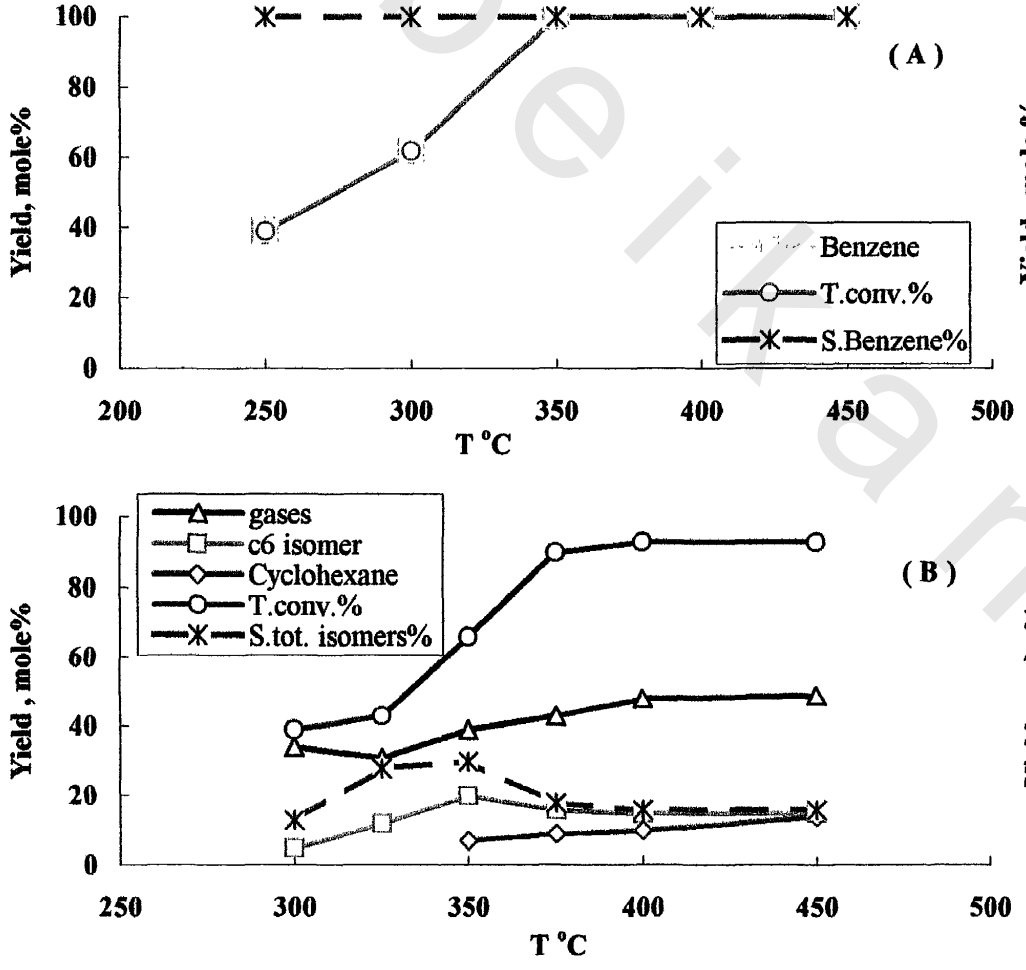

Fig. 49 The catalytic conversion of (A) cyclohexane (B) n-hexane over 0.3 wt% Pt/AlSBA-15(14)

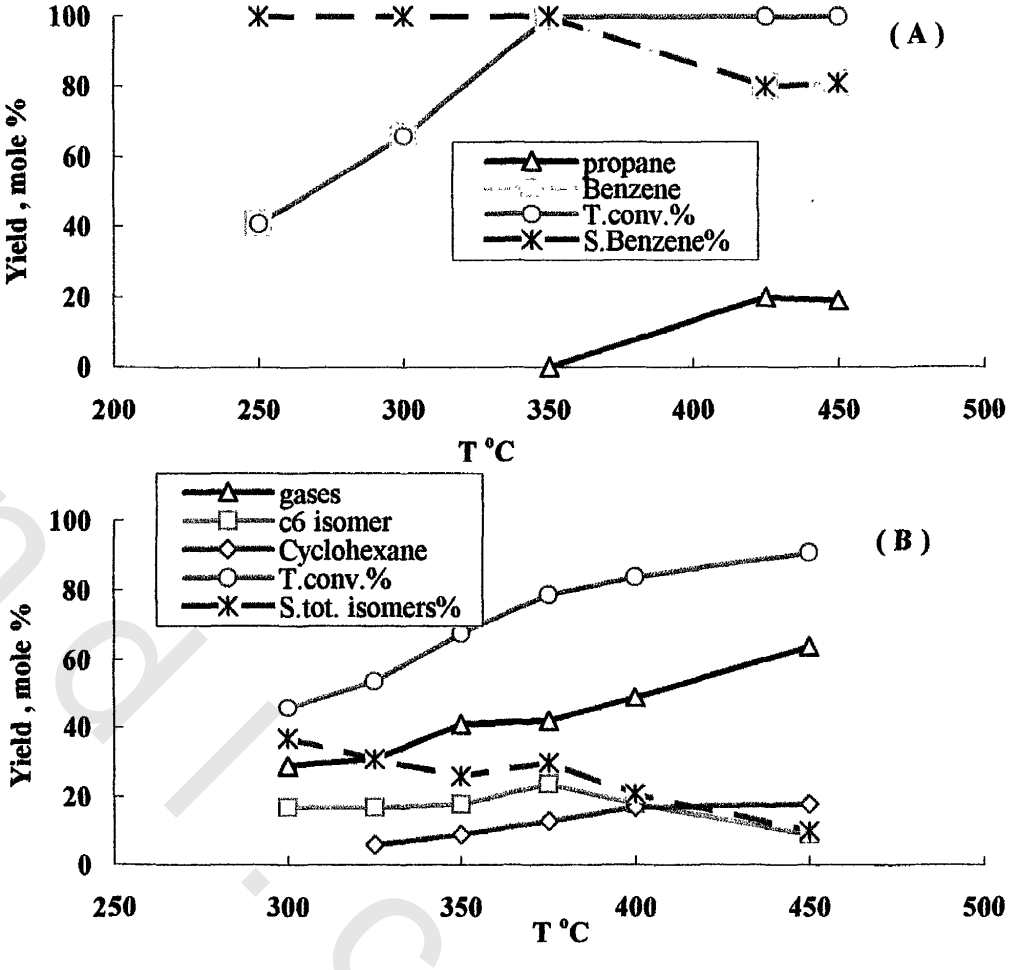

Fig. 50 The catalytic conversion of (A) cyclohexane (B) n-hexane over 0.6 wt% Pt/AlSBA-15 (14)

Table 16: Catalytic conversion of cyclohexane over Pt /AlSBA-15 (14) catalysts: (A) 0.3 wt%Pt and (B) 0.6 wt%Pt

Reaction products	Reaction temperature, °C				
	250	300	350	400	450
(A) Benzene	39	62	100	100	100
Cyclohexane	61	38	0	0	0
T.Conv. %	39	62	100	100	100
S.Benzene%	100	100	100	100	100
(B) propane	0	0	0	20	19
Benzene	41	66	100	80	81
Cyclohexane	59	34	0	0	0
T.Conv. %	41	66	100	100	100
S.Benzene%	100	100	100	80	81

Table 17: Catalytic conversion of n-hexane over Pt /AlSBA-15 (14) catalysts: (A) 0.3 wt%Pt and (B) 0.6 wt%Pt

Reaction products	Reaction temperature, °C					
	300	325	350	375	400	450
(A) gases	34	31	39	43	48	49
C_6 isomer	5	4	11	10	7	7
C_6	61	57	34	32	27	22
Mecyclopentane	0	8	9	6	8	8
Cyclohexane	0	0	7	9	10	14
T.Conv. %	39	43	66	90	93	93
S. tot. isomers%	13	28	30	18	16	16
(B) gases	29	31	41	42	49	64
C_6 isomer	11	13	11	17	11	9
C_6	54	46	32	21	16	9
Mecyclopentane	6	4	7	7	7	0
Cyclohexane	0	6	9	13	17	18
T.Conv. %	46	54	68	79	84	91
S. tot. isomers%	37	31	26	30	21	10

increasing reaction temperature and increases with increases Platinum concentration (Figs. 49 and 50-B).Beside isomer products, cracking gases and cyclohexane are formed. The yield of gases and cyclohexane increases by temperature and platinum loading.

III.2.4.6. Catalytic activity of Ni/AlSBA-15 (14) catalysts

(A) Cyclohexane conversion

Catalytic conversion of cyclohexane over Ni/AlSBA-15 catalysts with 2.5 and 7.5 wt%Ni (Figs.51 and 52-A) and Table 18 reveals both cracking and dehydrogenation pathways. The dehydrogenation of cyclohexane to benzene is, more or less, the same (±2) for Ni/AlSBA-15 catalyst sample containing 2.5 and 7.5 wt%Ni. The mole % of benzene increases with temperature reaching a maximum at 300 °C and then declines due to increasing yield of gaseous cracking products on the expense of benzene formation. At 300 °C, the mole % of benzene decreases by nickel loading for the sample containing 2.5 wt% (40%) but it decreases relatively for the sample containing 7.5 wt% Ni (38%). The yield of gases due to cracking increases with increasing both reaction temperature and nickel loading. The dehydrogenation selectivity decreases as nickel loading increases. The selectivity decreases sharply to rather low values at higher temperatures.

(B) n-hexane conversion

The catalytic conversion of n-hexane over Ni/SBA-15 catalysts with different Ni loading (2.5 and 7.5 wt% Ni) was shown in Figs.51 and 52 -B and Table 19.

n-hexane cracking into propane shows the highest yield in comparison with other cracking products, which reaches ~ 100 yields at 400 °C for both Ni loadings. The yield of propane increases with increasing both reaction temperature and nickel loading.

At lower temperature≤ 250 °C n-hexane is catalytically converted into methane, ethane, butane, and pentane whose yield increases with both reaction temperature and Ni loading.

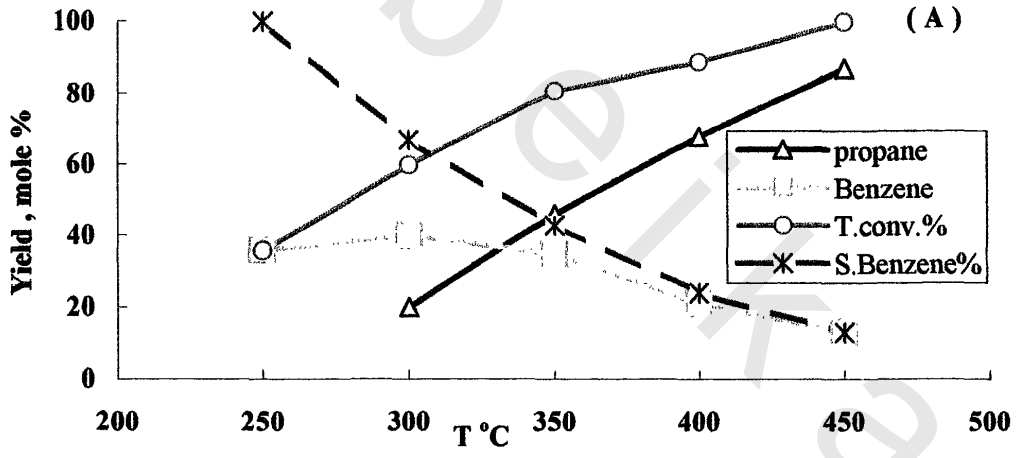

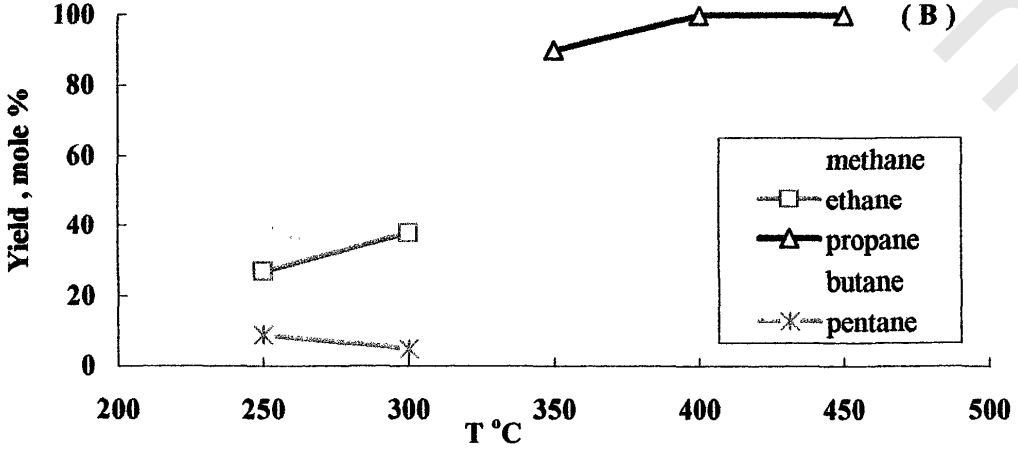

Fig. 51 The catalytic conversion of (A) cyclohexane (B) n-hexane over 2.5 wt% Ni/AlSBA-15 (14)

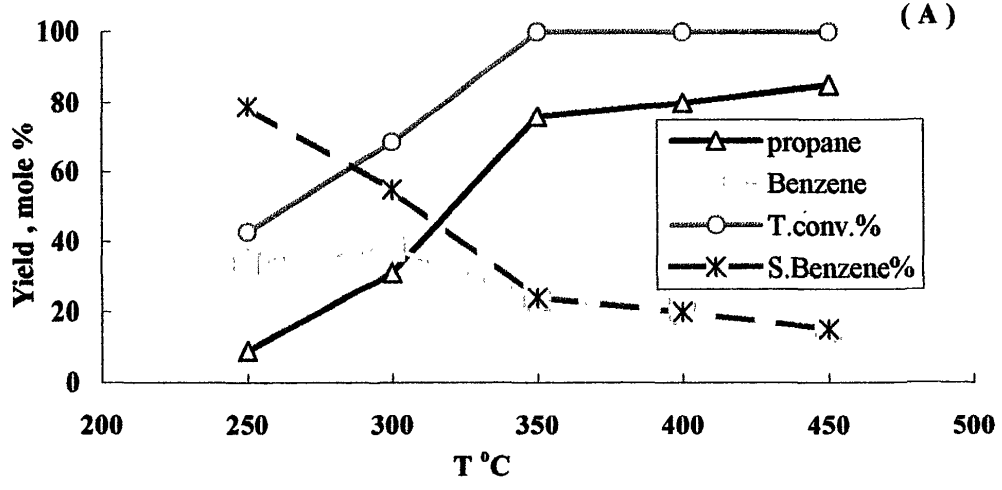

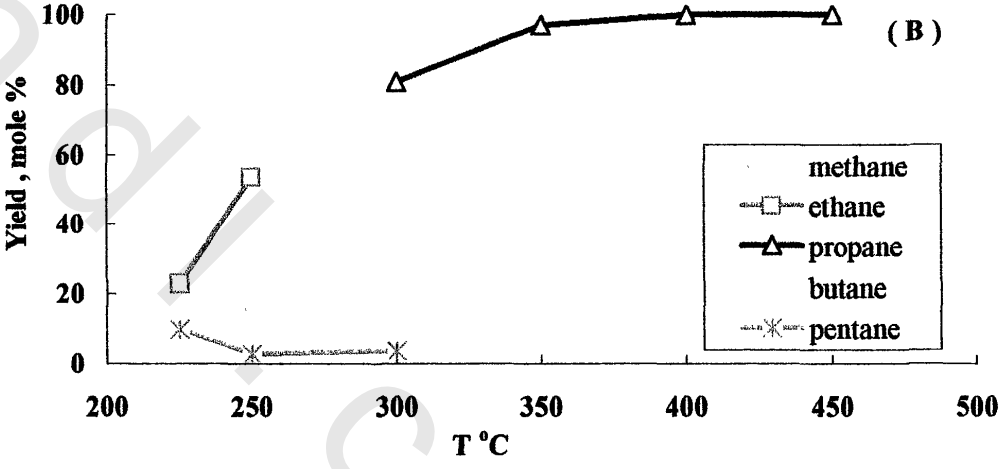

Fig. 52 The catalytic conversion of (A) cyclohexane (B) n-hexane over 7.5 wt % Ni/AlSBA-15 (14)

Table 18: Catalytic conversion of cyclohexane over Ni /AlSBA-15 (14) catalysts: (A) 2.5 wt%Ni and (B) 7.5 wt%Ni

Reaction products	Reaction temperature, °C				
	250	300	350	400	450
(A) propane	0	20	46	68	87
Benzene	36	40	35	21	13
Cyclohexane	64	40	19	11	0
T.Conv. %	36	60	81	89	100
S.Benzene%	100	67	43	24	13
(B) propane	9	31	76	80	85
Benzene	34	38	24	20	15
Cyclohexane	57	31	0	0	0
T.Conv. %	43	69	100	100	100
S.Benzene%	79	55	24	20	15

Table 19: Catalytic conversion of n-hexane over Ni /AlSBA-15 (14) catalysts: (A) 2.5 wt%Ni and (B) 7.5 wt%Ni

Reaction products	Reaction temperature, °C				
	250	300	350	400	450
(A) methane	40	24	0	0	0
ethane	27	38	0	0	0
propane	0	0	90	100	100
butane	14	20	0	0	0
pentane	9	5	0	0	0
n-hexane	10	13	10	0	0
(B) methane	12	0	0	0	0
ethane	54	0	0	0	0
propane	0	81	97	100	100
butane	28	0	0	0	0
pentane	3	4	0	0	0
n-hexane	3	15	3	0	0

From the above mentioned discussion, it may be concluded that:

-In general, Pt/AlSBA-15 (5, 7 and 14) catalysts are active ones toward cyclohexane dehydrogenation to benzene with higher yield, which occurred mainly on Pt metallic particles. Comparing the dehydrogenation activities of Pt/AlSBA-15 (5, 7 and 14), it was evident that the activity is arranged in the order, AlSBA-15(5) (0.3wt% > 0.6wt %) > AlSBA-15(14) (0.3wt% > 0.6wt %) > AlSBA-15(7) (0.6wt% > %0.3wt %). This is due to the appearance of propane as a result of cyclohexane cracking side reaction product at high temperature at the expense of benzene formation in case of Pt/AlSBA-15(7 and 14).

-Isomerization of n-hexane takes place over Pt/AlSBA-15 (5, 7 and 14) catalysts decreases with the increase of n_{Si}/n_{Al} ratio of the catalyst support in the order: Pt/AlSBA-15 (5) (0.3wt % > 0.6wt %) > Pt/AlSBA-15 (7) (0.3wt % > 0.6 wt %) > Pt/AlSBA-15 (14) (0.6wt % > %0.3wt %). This may explained by the proper balance between acid sites and metal sites of the support.

-The low yield of cyclohexane dehydrogenation to benzene and high yield of n-hexane cracking mainly into propane were observed over Ni/AlSBA15 (5, 7 and 14) catalysts. This type of catalysts exhibits higher cracking activity, being increased by increasing the nickel loading and reaction temperature. This may be due to after nickel impregnation, the Brønsted acid sites of AlSBA-15(5, 7 and 14) decreased while the lewis acid sites largely increased.[149] The nickel modification over the acidity of the support had two different effects.[150–152] On the one hand, the Ni species could cover some acid sites (both Brønsted and Lewis acid sites), causing the decrease of the total acid sites. On the other hand, the coordinately unsaturated nickel cations could serve as a kind of new Lewis acid centers, which compensated the original covered Lewis acid sites which cause the highly cracking activity of Ni/AlSBA-15(5, 7 and 14) catalysts thus much less dehydrogenation activity may be referred to the exposed nickel species as a result of the formation of strong interaction phase, namely Ni-Al-Si-OH (as evidenced by XRD measurements).